URLs. The February 2009 human reference sequence (GRCh37) produced by the Genome Reference Consortium was used as the reference genome (UCSC Genome Browser; http://genome.ucsc.edu/cgi-bin/hgGateway). Basewise conservation scores were calculated using PhyloP in the UCSC Genome Browser. Expression array and methylation array data were extracted from Oncomine (https://www.oncomine.org/), BioGPS (http://biogps.org/) and The Cancer Genome Atlas (TCGA; http://cancergenome.nih.gov/) and were analyzed by Matlab software (http://www.mathworks.com/). Somatic mutation data were searched in the Catalogue of Somatic Mutations in Cancer (COSMIC) database on the Welcome Trust Sanger Institute website (http://www.sanger.ac.uk/genetics/CGP/cosmic/). Each potential mutation was compared against databases of known SNPs, including Entrez Gene (http://www.ncbi.nlm.nih.gov/gene) and the Ensembl Genome Browser (http://useast.ensembl.org/index.html). SAMtools (http://samtools.sourceforge.net/) and Integrative Genomics Viewer (http://www.broadinstitute.org/igv/) software were used. The Database of Genomic Variants is a publically available database of copy number variations (http://projects.tcag.ca/variation).

METHODS

Methods and any associated references are available in the online version of the paper.

Accession codes. Whole-exome sequencing results have been deposited in the Sequence Read Archive (SRA; BioProject accession PRJNA203580).

Note: Supplementary information is available in the online version of the paper.

ACKNOWLEDGMENTS

We thank T. Yamaguchi (The University of Tokyo) for providing CS-Ubc lentivirus vector. This work was supported by US National Institutes of Health (NIH) grants RO1 HL-082983 (J.P.M.), U54 RR019391 (J.P.M.), K24 HL-077522 (J.P.M.) and RO1 CA-143193 (Y.D.), by a grant from the AA & MDS International Foundation, by the Robert Duggan Charitable Fund (J.P.M.), by a Scott Hamilton CARES grant (H. Makishima) and by Grants-in-Aid from the Ministry of Health, Labor and Welfare of Japan and KAKENHI (23249052, 22134006 and 21790907; S.O.), the project for the development of innovative research on cancer therapies (p-direct; S.O.), the Japan Society for the Promotion of Science (JSPS) through the Funding Program for World-Leading Innovative R&D on Science and Technology, initiated by the Council for Science and Technology Policy (CSTP; S.O.), NHRI-EX100-10003NI Taiwan (L.-Y.S.) and Uniformed Services University of the Health Sciences Pediatrics grant KM86GI (Y.D.). The results presented here are partly based on data generated by The Cancer Genome Atlas (TCGA) pilot project established by the National Cancer Institute and the National Human Genome Research Institute. Information about TCGA and the investigators and institutions that constitute the TCGA research network can be found at http://cancergenome.nih.gov/.

AUTHOR CONTRIBUTIONS

H. Makishima and K.Y. designed research, performed research, collected data, performed statistical analysis and wrote the manuscript. Y.O., N.N., K.P.N., B.P., K.O.G., B.A.V., A.J., I.G.-S., Y. Shiraishi, Y.N., M.S., M.T., K.C., H.T., H. Muramatsu, H.S., S.M. and L.-Y.S. performed research and analyzed data. K.G. and H. Mori collected data. M.A.S., R.L.P., M.A.M., S.K. and Y. Sauntharajah designed research, analyzed and interpreted data, and wrote the manuscript. Y.D., S.O. and J.P.M. designed research, contributed analytical tools, collected data, analyzed and interpreted data, and wrote the manuscript.

COMPETING FINANCIAL INTERESTS

The authors declare no competing financial interests.

1. Piazza, R. *et al.* Recurrent *SETBP1* mutations in atypical chronic myeloid leukemia. *Nat. Genet.* **45**, 18–24 (2013).
2. Hoischen, A. *et al. De novo* mutations of *SETBP1* cause Schinzel-Giedion syndrome. *Nat. Genet.* **42**, 483–485 (2010).
3. Damm, F. *et al. SETBP1* mutations in 658 patients with myelodysplastic syndromes, chronic myelomonocytic leukemia and secondary acute myeloid leukemias. *Leukemia* **27**, 1401–1403 (2013).
4. Laborde, R.R. *et al. SETBP1* mutations in 415 patients with primary myelofibrosis or chronic myelomonocytic leukemia (CMML): independent prognostic impact in CMML. *Leukemia* published online; doi:10.1038/leu.2013.97 (5 April 2013).
5. Thol, F. *et al. SETBP1* mutation analysis in 944 patients with MDS and AML. *Leukemia* published online; doi:10.1038/leu.2013.145 (7 May 2013).
6. Osato, M. *et al.* Biallelic and heterozygous point mutations in the runt domain of the AML1/PEBP2αB gene associated with myeloblastic leukemias. *Blood* **93**, 1817–1824 (1999).
7. Levine, R.L. *et al.* Activating mutation in the tyrosine kinase *JAK2* in polycythemia vera, essential thrombocythemia, and myeloid metaplasia with myelofibrosis. *Cancer Cell* **7**, 387–397 (2005).
8. Farr, C.J., Saiki, R.K., Erlich, H.A., McCormick, F. & Marshall, C.J. Analysis of *RAS* gene mutations in acute myeloid leukemia by polymerase chain reaction and oligonucleotide probes. *Proc. Natl. Acad. Sci. USA* **85**, 1629–1633 (1988).
9. Lyons, J., Janssen, J.W., Bartram, C., Layton, M. & Mufti, G.J. Mutation of Ki-*ras* and N-*ras* oncogenes in myelodysplastic syndromes. *Blood* **71**, 1707–1712 (1988).
10. Sanada, M. *et al.* Gain-of-function of mutated *C-CBL* tumour suppressor in myeloid neoplasms. *Nature* **460**, 904–908 (2009).
11. Delhommeau, F. *et al.* Mutation in *TET2* in myeloid cancers. *N. Engl. J. Med.* **360**, 2289–2301 (2009).
12. Ernst, T. *et al.* Inactivating mutations of the histone methyltransferase gene *EZH2* in myeloid disorders. *Nat. Genet.* **42**, 722–726 (2010).
13. Ley, T.J. *et al. DNMT3A* mutations in acute myeloid leukemia. *N. Engl. J. Med.* **363**, 2424–2433 (2010).
14. Mardis, E.R. *et al.* Recurring mutations found by sequencing an acute myeloid leukemia genome. *N. Engl. J. Med.* **361**, 1058–1066 (2009).
15. Yoshida, K. *et al.* Frequent pathway mutations of splicing machinery in myelodysplasia. *Nature* **478**, 64–69 (2011).
16. Papaemmanuil, E. *et al.* Somatic *SF3B1* mutation in myelodysplasia with ring sideroblasts. *N. Engl. J. Med.* **365**, 1384–1395 (2011).
17. Graubert, T.A. *et al.* Recurrent mutations in the *U2AF1* splicing factor in myelodysplastic syndromes. *Nat. Genet.* **44**, 53–57 (2012).
18. Walter, M.J. *et al.* Clonal architecture of secondary acute myeloid leukemia. *N. Engl. J. Med.* **366**, 1090–1098 (2012).
19. Walter, M.J. *et al.* Clonal diversity of recurrently mutated genes in myelodysplastic syndromes. *Leukemia* **27**, 1275–1282 (2013).
20. Minakuchi, M. *et al.* Identification and characterization of SEB, a novel protein that binds to the acute undifferentiated leukemia–associated protein SET. *Eur. J. Biochem.* **268**, 1340–1351 (2001).
21. Cristóbal, I. *et al.* SETBP1 overexpression is a novel leukemogenic mechanism that predicts adverse outcome in elderly patients with acute myeloid leukemia. *Blood* **115**, 615–625 (2010).
22. Ott, M.G. *et al.* Correction of X-linked chronic granulomatous disease by gene therapy, augmented by insertional activation of *MDS1-EVI1*, *PRDM16* or *SETBP1*. *Nat. Med.* **12**, 401–409 (2006).
23. Schinzel, A. & Giedion, A. A syndrome of severe midface retraction, multiple skull anomalies, clubfeet, and cardiac and renal malformations in sibs. *Am. J. Med. Genet.* **1**, 361–375 (1978).
24. Rodríguez, J.I., Jimenez-Heffernan, J.A. & Leal, J. Schinzel-Giedion syndrome: autopsy report and additional clinical manifestations. *Am. J. Med. Genet.* **53**, 374–377 (1994).
25. Pardanani, A. *et al. CSF3R* T618I is a highly prevalent and specific mutation in chronic neutrophilic leukemia. *Leukemia* published online; doi:10.1038/leu.2013.122 (22 April 2013).
26. Meggendorfer, M. *et al. SETBP1* mutations occur in 9% of MDS/MPN and in 4% of MPN cases and are strongly associated with atypical CML, monosomy 7, isochromosome i(17)(q10), *ASXL1* and *CBL* mutations. *Leukemia* published online; doi:10.1038/leu.2013.133 (30 April 2013).
27. Makishima, H. *et al. CBL* mutation–related patterns of phosphorylation and sensitivity to tyrosine kinase inhibitors. *Leukemia* **26**, 1547–1554 (2012).
28. Sakaguchi, H. *et al.* Exome sequencing identifies secondary mutations of *SETBP1* and *JAK3* in juvenile myelomonocytic leukemia. *Nat. Genet.* published online; doi:10.1038/ng.2698 (7 July 2013).
29. Goyama, S. *et al.* Evi-1 is a critical regulator for hematopoietic stem cells and transformed leukemic cells. *Cell Stem Cell* **3**, 207–220 (2008).
30. Greenberg, P. *et al.* International scoring system for evaluating prognosis in myelodysplastic syndromes. *Blood* **89**, 2079–2088 (1997).
31. Oakley, K. *et al. Setbp1* promotes the self-renewal of murine myeloid progenitors via activation of *Hoxa9* and *Hoxa10*. *Blood* **119**, 6099–6108 (2012).
32. Cohen, S.B., Zheng, G., Heyman, H.C. & Stavnezer, E. Heterodimers of the SnoN and Ski oncoproteins form preferentially over homodimers and are more potent transforming agents. *Nucleic Acids Res.* **27**, 1006–1014 (1999).
33. Cristóbal, I. *et al.* PP2A impaired activity is a common event in acute myeloid leukemia and its activation by forskolin has a potent anti-leukemic effect. *Leukemia* **25**, 606–614 (2011).

ONLINE METHODS

Subject population. Bone marrow aspirates or blood samples were collected from 727 individuals with various myeloid malignancies seen at the Cleveland Clinic, the University of Tokyo, the University of California, Los Angeles, the Sidney Kimmel Comprehensive Cancer Center at Johns Hopkins, Chang Gung University and Showa University (**Supplementary Table 6**). Informed consent for sample collection was obtained according to protocols approved by the institutional review board at each participating institute and in accordance with the Declaration of Helsinki. Diagnosis was confirmed and assigned according to World Health Organization (WHO) classification criteria[34]. Prognostic risk assessment was assigned according to the International Scoring Criteria for individuals with MDS and chronic myelomonocytic leukemia with a white cell count of <12,000 cells/μl[30]. For the purpose of this study, low-risk MDS was defined as having <5% myeloblasts. Individuals with ≥5% myeloblasts constituted those with higher risk disease. Serial samples were obtained for 12 individuals with *SETBP1* mutations. As a source of germline controls, immunoselected $CD3^+$ T lymphocytes were used in an additional nine cases. Cytogenetic analysis was performed according to standard banding techniques on the basis of 20 metaphases, if available. Clinical parameters studied included age, sex, overall survival, bone marrow blast counts and metaphase cytogenetics.

Cytogenetics and SNP arrays. Technical details regarding sample processing for SNP array assays were previously described[35,36]. The Gene Chip Mapping 250K Assay kit and the Genome-Wide Human SNP Array 6.0 (Affymetrix) were used. A stringent algorithm was applied for the identification of lesions using SNP arrays. Individuals with lesions identified by SNP array concordant with those identified in metaphase cytogenetics or typical lesions known to be recurrent required no further analysis. Changes reported in our internal or publicly available (Database of Genomic Variants; see URLs) copy number variation (CNV) databases were considered non-somatic and were excluded. Results were analyzed using CNAG (v3.0)[37] or Genotyping Console (Affymetrix). All other lesions were confirmed as somatic or germline by analysis of CD3-sorted cells[38].

Whole-exome sequencing. Whole-exome sequencing was performed as previously reported[15]. Briefly, tumor DNA was extracted from bone marrow or peripheral blood mononuclear cells from affected individuals. For germline controls, DNA was obtained from paired $CD3^+$ T cells. Whole-exome capture was accomplished using liquid-phase hybridization of sonicated genomic DNA with mean length of 150–200 bp to the bait cRNA library synthesized on magnetic beads (SureSelect, Agilent Technologies) according to the manufacturer's protocol. The SureSelect Human All Exon 50Mb kit was used for 20 cases (**Supplementary Table 1**). Captured targets were subjected to massive sequencing using the Illumina HiSeq 2000 platform with the paired-end 75- to 108-bp read option, according to the manufacturer's instructions. Raw sequence data generated from HiSeq 2000 sequencers were processed through the in-house pipeline constructed for the whole-exome analysis of paired cancer genomes at the Human Genome Center, Institute of Medical Science, University of Tokyo, which is summarized in a previous report[15]. Data processing is divided into two steps: (i) generation of a BAM file (using SAMtools) for paired normal and tumor samples for each case and (ii) detection of somatic SNVs and indels by comparing normal and tumor BAM files. Alignment of sequencing reads on the hg19 reference genome was visualized using Integrative Genomics Viewer (IGV) software[39].

For all candidate somatic mutations, the accuracy of the prediction of these SNVs and indels by whole-exome sequencing was tested by validation of 65 genes (80 events) by Sanger sequencing and targeted deep sequencing. Prediction had a true positive rate of 47% (39% for missense mutation, 75% for nonsense mutations and 75% for indels). It is of note that prediction of known somatic mutations (for example, in *TET2* ($n = 9$), *CBL* ($n = 2$), *SETBP1* ($n = 2$) and *ASXL1* ($n = 2$)) showed accuracy of 100% (**Supplementary Tables 2–4**).

Targeted deep sequencing. To detect allelic frequencies for mutations or SNPs, we applied deep sequencing to targeted exons as previously described[15]. Briefly, we screened for possible mutations of *SETBP1* and other genes that were concomitantly mutated in the cases with *SETBP1* mutation (*U2AF1*, *DNMT3A*, *NRAS*, *ASXL1*, *SRSF2*, *CBL*, *IDH1*, *IDH2*, *SRSF2*, *TET2*, *PTPN11* and *RUNX1*). Each targeted exon was amplified with NotI linker attached to each primer as previously described[15]. After digestion with NotI, amplicons were ligated with T4 DNA ligase and sonicated into fragments that were on average up to 200 bp in size using Covaris. Sequencing libraries were generated according to an Illumina paired-end library protocol and were subjected to deep sequencing on the Illumina Genome Analyzer IIx or HiSeq 2000 sequencers according to the standard protocol.

Sanger sequencing and allele-specific PCR. Exons of selected genes were amplified and underwent direct genomic sequencing by standard techniques on the ABI 3730xl DNA analyzer (Applied Biosystems) as previously described[40–42]. Coding and sequenced exons are shown in **Supplementary Table 8**. All mutations were detected by bidirectional sequencing and were scored as pathogenic if not present in non-clonal paired DNA from CD3-selected cells. When a mutant allele with small burden was not confirmed by Sanger sequencing, cloning and sequencing of individual colonies (TOPO TA cloning, Invitrogen) was performed for validation. The allelic presence of p.Asp868Asn and p.Gly870Ser alterations was determined by allele-specific PCR. Primer sequences for *SETBP1* sequencing and *SETBP1* allele-specific PCR are provided in **Supplementary Table 14**.

Quantitative RT-PCR using TaqMan probes. Total RNA was extracted from bone marrow mononuclear cells and cell lines. cDNA was synthesized from 500 ng of total RNA using the iScript cDNA synthesis kit (Bio-Rad). Quantitative gene expression levels were detected using RT-PCR with the ABI PRISM 7500 Fast Sequence Detection System and FAM dye–labeled TaqMan MGB probes (Applied Biosystems). TaqMan probes for all genes analyzed were gene expression assay products purchased from Applied Biosystems (*SETBP1*, Hs00210209_m1; *HOXA9*, Hs00365956_m1; *HOXA10*, Hs00172012_m1; *GAPDH*, Hs99999905_m1). Expression levels of target genes were normalized to *GAPDH* mRNA levels.

Retrovirus generation. pMYs-*Setbp1* retrovirus expressing 3× Flag–tagged wild-type Setbp1 protein and green fluorescent protein (GFP) marker was described previously[31]. Point mutations of *Setbp1* (encoding p.Asp868Asn and p.Ile871Thr alterations) were generated using the same construct and the QuickChange II Site-Directed Mutagenesis kit (Agilent Technologies). Virus was produced by transient transfection of Plat-E cells (Cell Biolabs) using FuGene 6 (Roche). Viral titers were calculated by infecting NIH3T3 cells with serially diluted viral stock and counting GFP-positive colonies 48 h after infection.

Immortalization of myeloid progenitors. Immortalization of myeloid progenitors was performed as described according to protocols approved by the Institutional Animal Care and Use Committee of the Uniformed Services University of the Health Sciences[31]. Briefly, whole–bone marrow cells harvested from three young C57BL/6 mice were first cultured in StemSpan medium (Stemcell Technologies) with 10 ng/ml mouse SCF, 20 ng/ml mouse TPO, 20 ng/ml mouse IGF-2 (all from R&D Systems) and 10 ng/ml human FGF-1 (Invitrogen) for 6 d to expand primitive stem and progenitor cells. Myeloid differentiation was subsequently induced by growing the expanded cells in IMDM supplemented with 20% heat-inactivated horse serum with 100 ng/ml mouse SCF (PeproTech) and 10 ng/ml mouse IL-3 for 4 d. Resulting cells (5×10^5) were infected with retrovirus (1×10^5 colony-forming units (CFUs)) on plates coated with Retronectin (Takara) for 48 h. Infected cells were then continuously passaged at a 1:10 ratio every 3 d for 4 weeks to test whether transduction caused immortalization of the myeloid progenitors. In the absence of immortalization, transduced cultures generally ceased expanding in 2 weeks.

Methylation analysis. The DNA methylation status of bisulfite-treated genomic DNA was probed at 27,578 CpG dinucleotides using the Illumina Infinium HumanMethylation 27k BeadChip assay as previously described[43]. Briefly, methylation status was calculated from the ratio of methylation-specific and demethylation-specific fluorophores (β value) using the BeadStudio Methylation Module (Illumina).

Resistance of SETBP1 protein degradation associated with *SETBP1* mutation. Full-length wild-type human *SETBP1* cDNA encoding 3× HA–tagged protein was cloned from peripheral blood mononuclear cells. Mutagenesis of *SETBP1* (to introduce mutations encoding the p.Asp868Asn and p.Ile871Thr alterations) was performed using the PrimeSTAR kit (Takara Bio). Wild-type and mutant cDNA constructs were cloned into the CS-Ubc lentivirus vector (a kind gift of T. Yamaguchi). Vectors were cotransfected with packaging vector and with vectors expressing VSV-G and Rev into 293T cells, and lentiviral particles were harvested. Protein blotting experiments on whole lysates from Jurkat cell line stably transduced with viruses expressing wild-type and mutant SETBP1 were carried out with antibodies for HA at a 1:2,000 dilution (MMS-101R, Covance) and actin at a 1:1,000 dilution (sc-1616, Santa Cruz Biotechnology). Both cell lines were obtained from ATCC. For proteasomal inhibition, cell lines were treated with 0.5 μM lactacystin (Peptide Institute) and 0.25 μM bafilomycin A1 (Wako Junyaku) for 2 h.

Statistical analysis. The Kaplan-Meier method was used to analyze survival outcomes (overall survival) by the log-rank test. Pairwise comparisons were performed by Wilcoxon test for continuous variables and by two-sided Fisher's exact test for categorical variables. Paired data were analyzed by Wilcoxon signed-rank test. For multivariate analyses, a Cox proportional hazards model was conducted for overall survival. Variables considered for model inclusion were IPSS risk group, age, sex and gene mutation status. Variables with $P < 0.05$ in univariate analyses were included in the model. Statistical analyses were performed with JMP9 software (SAS). Significance was determined at a two-sided α level of 0.05, except for P values in multiple comparisons, in which Bonferroni correction was applied.

34. Shaffer, L.G. & Tommerup, N. *ISCN 2009. An International System for Human Cytogenetics Nomenclature* (Karger, Basel, Switzerland, 2009).
35. Maciejewski, J.P., Tiu, R.V. & O'Keefe, C. Application of array-based whole genome scanning technologies as a cytogenetic tool in haematological malignancies. *Br. J. Haematol.* **146**, 479–488 (2009).
36. Gondek, L.P. *et al.* Chromosomal lesions and uniparental disomy detected by SNP arrays in MDS, MDS/MPD, and MDS-derived AML. *Blood* **111**, 1534–1542 (2008).
37. Nannya, Y. *et al.* A robust algorithm for copy number detection using high-density oligonucleotide single nucleotide polymorphism genotyping arrays. *Cancer Res.* **65**, 6071–6079 (2005).
38. Tiu, R.V. *et al.* New lesions detected by single nucleotide polymorphism array–based chromosomal analysis have important clinical impact in acute myeloid leukemia. *J. Clin. Oncol.* **27**, 5219–5226 (2009).
39. Robinson, J.T. *et al.* Integrative genomics viewer. *Nat. Biotechnol.* **29**, 24–26 (2011).
40. Dunbar, A.J. *et al.* 250K single nucleotide polymorphism array karyotyping identifies acquired uniparental disomy and homozygous mutations, including novel missense substitutions of *c-Cbl*, in myeloid malignancies. *Cancer Res.* **68**, 10349–10357 (2008).
41. Jankowska, A.M. *et al.* Loss of heterozygosity 4q24 and *TET2* mutations associated with myelodysplastic/myeloproliferative neoplasms. *Blood* **113**, 6403–6410 (2009).
42. Makishima, H. *et al. CBL*, *CBLB*, *TET2*, *ASXL1*, and *IDH1/2* mutations and additional chromosomal aberrations constitute molecular events in chronic myelogenous leukemia. *Blood* **117**, e198–e206 (2011).
43. Ko, M. *et al.* Impaired hydroxylation of 5-methylcytosine in myeloid cancers with mutant *TET2*. *Nature* **468**, 839–843 (2010).

Leukemia Research 38 (2014) 42–48

Contents lists available at ScienceDirect

Leukemia Research

journal homepage: www.elsevier.com/locate/leukres

Significance of CD66c expression in childhood acute lymphoblastic leukemia

Nobutaka Kiyokawa[a,*,1], Kazutoshi Iijima[a], Osamu Tomita[a,1], Masashi Miharu[a,b,1], Daisuke Hasegawa[a,c,1], Kenichiro Kobayashi[a], Hajime Okita[a], Michiko Kajiwara[d,1], Hiroyuki Shimada[b,1], Takeshi Inukai[e,1], Atsushi Makimoto[f,1], Takashi Fukushima[g,1], Toru Nanmoku[h], Katsuyoshi Koh[i,1], Atsushi Manabe[c,1], Akira Kikuchi[j,1], Kanji Sugita[e,1], Junichiro Fujimoto[k,1], Yasuhide Hayashi[l,1], Akira Ohara[m,1]

[a] Department of Pediatric Hematology and Oncology Research, National Research Institute for Child Health and Development, Setagaya-ku, Tokyo, Japan
[b] Department of Pediatrics, Keio University School of Medicine, Shinjuku-ku, Tokyo, Japan
[c] Department of Pediatrics, St. Luke's International Hospital, Chuo-ku, Tokyo, Japan
[d] Department of Transfusion Medicine, Medical Hospital, Tokyo Medical and Dental University, Bunkyo-ku, Tokyo, Japan
[e] Department of Pediatrics, School of Medicine, University of Yamanashi, Chuo, Yamanashi, Japan
[f] Division of Pediatric Oncology, National Cancer Center Hospital, Chuo-ku, Tokyo, Japan
[g] Department of Child Health, Faculty of Medicine, University of Tsukuba, Tsukuba, Ibaraki, Japan
[h] Department of Clinical Laboratory, University of Tsukuba Hospital, Tsukuba, Ibaraki, Japan
[i] Department of Hematology/Oncology, Saitama Children's Medical Center, Saitama, Saitama, Japan
[j] Department of Pediatrics, Teikyo University School of Medicine, Itabashi-ku, Tokyo, Japan
[k] Clinical Research Center, National Center for Child Health and Development, Setagaya-ku, Tokyo, Japan
[l] Department of Hematology-Oncology, Gunma Children's Medical Center, Shibukawa, Gunma, Japan
[m] Department of Pediatrics, Toho University Omori Medical Center, Ota-ku, Tokyo, Japan

ARTICLE INFO

Article history:
Received 17 December 2012
Received in revised form
29 September 2013
Accepted 13 October 2013
Available online 22 October 2013

Keywords:
CD66c
Acute lymphoblastic leukemia
CRLF2, Flow cytometry
Genetic abnormality

ABSTRACT

Upon analyzing 696 childhood B-cell precursor acute lymphoblastic leukemia (BCP-ALL) cases, we identified the characteristics of CD66c expression. In addition to the confirmation of strong correlation with *BCR-ABL* positivity and hyperdiploid, we further observed that CD66c is frequently expressed in CRLF2-positive (11/15, $p < 0.01$ against chimeric gene-negative) as well as hypodiploid cases (3/4), whereas it is never expressed in *ETV6-RUNX1*, *MLL-AF4*, *MLL-AF9*, *MLL-ENL*, and *E2A-PBX1*-positive cases. Although the expression of CD66c itself is not directly linked to the prognosis, the accompanying genetic abnormalities are important prognostic factors for BCP-ALL, indicating the importance of CD66c expression in the initial diagnosis of BCP-ALL.

1. Introduction

Although most leukemic cells retain the characteristics of their normal counterparts and exhibit commitment to any one of the hematopoietic lineages, they frequently show lineage-uncommitted antigen expression, referred to as "aberrant antigen expression" or "lineage infidelity". For example, both T-cell and B-cell precursor (BCP) acute lymphoblastic leukemia (ALL) cells commonly express aberrant myeloid lineage antigens, while acute myeloid leukemia (AML) cells often exhibit the expression of T- or B-cell lineage antigens. Several possibilities to explain this phenomenon have been postulated, whereas the precise mechanism is still unclear [1–3].

CD66c, also called CEACAM6, KOR-SA3544 antigen, and NCA 90/50, is a heavily glycosylated glycosylphosphatidylinositol (GPI)-anchored protein belonging to the carcinoembryonic antigen family, having two constant Ig-like domains and one variable Ig-like domain [4]. The expression of CD66c is observed only in granulocytes and its precursors among normal hematopoiesis [5], while it is known as the most frequently observed aberrant myeloid

* Corresponding author at: Department of Pediatric Hematology and Oncology Research, National Research Institute for Child Health and Development, 2-10-1, kura, Setagaya-ku, Tokyo 157-8535, Japan. Tel.: +81 3 3417 2496; fax: +81 3 3417 2496.
E-mail address: kiyokawa-n@ncchd.go.jp (N. Kiyokawa).
[1] From the Tokyo Children's Cancer Study Group.

0145-2126/$ – see front matter © 2013 Elsevier Ltd. All rights reserved.
http://dx.doi.org/10.1016/j.leukres.2013.10.008

Table 1
The summary of the characteristics of patients.

	n=	Age (mean ± SD)	Range	Initial WBC/μl (mean ± SD)	Range	Gender (male:female)	NCI risk group (SR:HR)
BCR-ABL	35	8.4 ± 4.1	2–15	141,950.0 ± 202,731.2	1220–881,700	0.60:0.40	0.80:0.20
MLL-chimera	20	5.5 ± 4.8	0–15	233,237.2 ± 336,648.4	3300–1,165,400	0.45:0.55	0.80:0.20
E2A-PBX1	65	6.5 ± 4.5	1–15	39,857.4 ± 44,938.8	1730–223,300	0.52:0.48	0.94:0.06
ETV6-RUNX1	154	4.8 ± 2.8	1–15	26,426.4 ± 73,112.6	1600–788,000	0.56:0.44	1.00:0.00
Neardiploid	267	6.1 ± 4.3	1–17	31,153.1 ± 71,020.0	700–597,000	0.53:0.47	0.96:0.04
CRLF2+	15	7.7 ± 4.7	1–16	95,105.5 ± 134,773.6	4200–368,700	0.60:0.40	0.93:0.07
Hypodiploid	4	7.3 ± 5.0	2–12	10,075.0 ± 7605.4	4900–23,200	0.75:0.25	1.00:0.00
Hyperdiploid	136	4.4 ± 2.9	1–15	14,256.6 ± 27,170.5	1100–259,000	0.54:0.46	1.00:0.00
Total	696	5.6 ± 3.9		39,318.0 ± 102,794.7	700–1,165,400	0.54:0.46	0.96:0.04
Neardiploid							
CD66c+	106	5.7 ± 3.8	1–15	24,402.5 ± 51,598.1	700–379,500	0.54:0.46	0.96:0.04
CD66c-	161	6.3 ± 4.6	1–17	35,555.7 ± 80,919.0	800–597,000	0.53:0.47	0.97:0.03
Hyperdiploid							
CD66c+	91	4.3 ± 2.4	1–12	12,339.3 ± 17,488.1	1100–116,900	0.58:0.42	1.00:0.00
CD66c-	45	4.5 ± 3.9	1–15	18,278.3 ± 40,265.9	1700–259,000	0.44:0.56	1.00:0.00

antigen in B-cell precursor acute lymphoblastic leukemia (BCP-ALL) [6]. CD66c was initially reported to be expressed highly selectively in *BCR-ABL*-positive BCP-ALL, while some *BCR-ABL*-negative cases also express this antigen [7]. Later, it was reported that CD66c was correlated strongly with *ETV6-RUNX1* and *MLL-AF4* negativity and was found at high levels in hyperdiploidy [6,8]. A number of studies to clarify the function of this molecule have been performed, and it has been reported that CD66c is involved in homo- and heterotypic adhesion [9], contributes to Ca2+-mediated signaling [10], and is involved in apoptosis induction [11]. However, the biological significance of this molecule in BCP-ALL is still not fully understood.

In an attempt to explore the significance of the expression of CD66c in BCP-ALL, we precisely characterized the properties of CD66c-positive ALL in a large cohort. In this study, we further extend previous findings and indicate that CD66c expression has a close correlation with a definite set of genetic abnormalities, although it is not limited to a specific one. The detection of CD66c at the initial diagnosis of BCP-ALL is important for the prediction of the presence and absence of certain genetic abnormalities. Although the expression of CD66c itself is not directly linked to the prognosis, the genetic abnormalities accompanying CD66c expression are important prognostic factors for BCP-ALL, and, thus, the genetic findings need to be investigated carefully with the presence of CD66c expression.

2. Materials and methods

2.1. Case selection

A total of 696 patients aged between 1 and 18 years (male: female; 0.54: 0.46) who had been newly diagnosed with BCP-ALL and consecutively enrolled on the Tokyo Children's Cancer Study Group (TCCSG) L16 study from December 2004 to August 2012 were included in this study. The characteristics of patients, including age, initial white blood cell (WBC) count, and NCI risk group, were summarized in Table 1. The investigations were approved by the institutional review boards of all participating institutions. Informed consent was obtained from parents or guardians, and informed assent was obtained from the patients when appropriate given their age and understanding.

Bone marrow (BM) and/or peripheral blood (PB) smears of the patients were stained by standard techniques, and the diagnosis of ALL was made according to the morphologic and cytochemical (myeloperoxidase and nonspecific esterase) criteria of the French-American-British (FAB) classification. All cases had fewer than 3% myeloperoxidase-positive, 3% Sudan black B-positive (myeloid pattern), or 20% butyrate esterase-positive (myeloid pattern) blast cells and no Auer rods. Basically, children with ALL of the mature B-cell type were not enrolled in this trial. BM aspirate or PB was immediately mixed with anti-coagulant and sent by overnight transport to the flow cytometry and fusion transcript laboratories, National Research Institute for Child Health and Development (NCH) and Univ. of Tsukuba, respectively, as part of routine pretreatment studies.

2.2. Flow cytometry

Four-color flow cytometric immunophenotyping with CD45-gating was performed on a flow cytometer (FC500, Beckman-Coulter, Brea, CA). The panel monoclonal antibodies (MoAbs) used for immunophenotyping are presented in Supplementary information. Whole blood samples were stained with various combinations of fluorescein isothiocyanate (FITC)-, phycoerythrin (PE)-, PE-cyanin 5.1 (PC5)-, and PE-cyanine 7 (PC7)-conjugated MoAbs in the presence of electron-coupled dye (ECD)-conjugated CD45, following RBC-lysis treatment. For the detection of cytoplasmic (cyCD3, cyCD22, cyCD79a, cy-μ, and MPO) and nuclear TdT antigens, the cells were permeabilized with the Intraprep Permeabilization reagent kit (Beckman-Coulter). Analysis was done by collecting 10,000 gated list mode events, and selecting an appropriate blast gate for the combination of CD45 and side scatter. An antigen was considered positively expressed when at least 20% of the gated cells expressed that antigen.

DNA contents were examined by Propidium Iodide (PI)-staining. Following RBC-lysis treatment, 2.5×10^5 cells were suspended in phosphate-buffered saline (PBS) containing 0.2% of Triton X-100, 20 μg/ml of PI, and 100 ng/ml of RNase (Sigma–Aldrich, St. Louis, MO). PI fluorescence was collected through a 645-nm dichroic long-pass filter and a 620-nm band-pass filter. Upon appropriate gating, at least 10,000 events were collected and analyzed.

The detection of BCR-ABL protein by flow cytometry was performed by Cytometric Bead Array (CBA) for BCR-ABL protein (Becton Dickinson, BD, Franklin Lakes, NJ) according to manufacturer's instruction.

2.3. Detection of fusion transcripts and conventional cytogenetic analysis

The expression of 8 fusion transcripts: *MLL-AF4*, *MLL-AF9*, *MLL-ENL*, major *BCR-ABL*, minor *bcr-abl*, *ETV6-RUNX1*, *E2A-PBX*, and *SIL-TAL1*, was detected by real-time PCR using appropriate primer sets. Cytogenetic analysis was performed on bone marrow or peripheral blood specimens using standard techniques. At least 20 metaphases were examined for each case. Actual examinations were performed by Special Reference Laboratory (SRL, Tachikawa, Tokyo, Japan). In the present study, we have defined BCP-ALL cases with more than 51 chromosomes or DNA-index > 1.16 (corresponding to 51 chromosomes) as hyperdiploid (high-hyperdiploid) based on the previous reports [12,13]. Similarly, we have defined the cases with fewer than 44 chromosomes [13–15] or DNA-index < 0.95 (corresponding to 43 chromosomes) [16] as hypodiploid (near-haploid, low-hypodiploid and high-hypodiploid). The cases with 44–50 chromosomes have designated as neardiploid.

2.4. Statistical analysis

Statistical analysis was performed by means of Student's *t*-test. A *p*-value less than 0.05 was considered significant. Principal components analysis (PCA) was performed by using TriSP version2.1 developed by Yamasaki H (http://www014.upp.so-net.ne.jp/acremaker/).

3. Results

3.1. Close correlation between CD66c expression and nonrandom genetic abnormalities

We analyzed CD66c expression in 696 unselected patients' specimens with a diagnosis of BCP-ALL and available information on the presence of well-established chimeric genes, including major and minor *BCR-ABL*, *ETV6-RUNX1*, *E2A-PBX1*, *MLL-AF4*, *MLL-AF9*, and *MLL-ENL* and/or cytogenetic findings, including DNA ploidy. As shown in Table 2, CD66c was expressed in 34.9% of all BCP-ALL cases

Table 2
Expression of myeloid antigens in B-cell precursor acute lymphoblastic leukemia.

	CD66c	CD33	CD13	CD15	CD65	CD117
>20% (%)	34.91	21.73	9.20	3.44	2.46	1.62
Number	(243/696)	(151/695)	(64/696)	(23/668)	(17/692)	(11/679)
Mean (%)	23.18	13.53	6.40	3.35	2.80	1.88
SD (%)	31.26	21.85	14.11	8.57	9.59	5.08
Median (%)	4.87	2.58	1.26	0.79	0.70	0.35

and appeared to be most frequently aberrantly expressed in BCP-ALL compared to other myeloid antigens, including CD33 (21.7%), CD13 (9.2%), CD15 (3.4%), CD65 (2.5%), and CD117 (1.6%).

Consistent with previous reports, CD66c expression showed a close correlation with nonrandom genetic abnormalities and was expressed only in *BCR-ABL*-positive (91.4%, 32/35) or specific chimeric gene-negative cases (50.0%, 211/422), while none of the *ETV6-RUNX1*-positive cases expressed CD66c (Fig. 1A). In addition, not only the *MLL-AF4*-positive cases, but also *MLL-AF9* and *MLL-ENL*-positive cases were negative for CD66c. Furthermore, it is noteworthy that none of the *E2A-PBX1*-positive cases expressed CD66c.

3.2. High rate expression of CD66c in CRLF2-positive and hyperdiploid cases

Next, we further analyzed CD66c expression in BCP-ALL cases without specific chimeric genes (Fig. 1B). The chimeric gene-negative BCP-ALL cases can be subdivided into near-, hyper-, and hypodiploid based on the number of chromosomes. The abnormalities in chromosome number have been shown to have prognostic significance in BCP-ALL and hyperdiploid ALL (more than 51 chromosomes) exhibit a superior outcome [12,13], whereas hypodiploid ALL (fewer than 44 chromosomes) is characterized by extremely poor outcomes when compared with their nonhyperdiploid counterparts (44–50 chromosomes) [13–15]. As shown in Fig. 1B, hyperdiploid cases exhibited high frequency of CD66c expression (66.9%, 91/136). Interestingly, although the number of cases was small, three out of four hypodiploid cases were positive for CD66c.

In our study, we examined the expression of CRLF2 using specific monoclonal antibody retrospectively and prospectively, and found 15 CRLF2-positive cases in the neardiploid cases (2.2% in our total cohort). As shown in Fig. 1B, CRLF2-positive cases exhibited a significantly high frequency of CD66c-expression and 73.3% (11/15) were CD66c-positive. No significant difference was observed between hyperdiploid and CRLF2-positive cases in CD66c-expression. In contrast, the remaining neardiploid cases exhibited less frequent CD66c-expression (39.7%, 106/267).

3.3. Correlation between CD66c expression and that of other myeloid antigens and CD21/CD27 expression

It was reported that the expression of myeloid antigens tended to be mutually exclusive with CD66c [6]. Therefore, we next examined the correlation between the expression of CD66c and other myeloid antigens. As presented above, BCP-ALL cases possessing specific chimeric genes except *BCR-ABL* never express CD66c. Since it was also reported that *ETV6-RUNX1*-positive ALL frequently expressed CD33 and CD13 [17], ALLs expressing these two antigens should be enriched in CD66c-negative/neardiploid cases. Therefore, we compared *BCR-ABL*-positive and chimeric gene-negative cases by excluding BCP-ALL cases possessing other specific chimeric genes from this analysis.

As shown in Fig. 2A and B, the expression of CD33 and CD13 was concentrated in *BCR-ABL*-positive and neardiploid cases. As described above, the vast majority of BCR-ABL-positive cases expressed CD66c and they exhibited a higher frequency of both CD33 (37.5%, 12/32) and CD13 (18.8%, 6/32) expression compared to CD66c-positive cases with neardiploid and hyperdiploid states. In contrast, although we excluded *ETV6-RUNX1*-positive cases from the analysis, neardiploid/CD66c-negative cases still exhibited a significantly higher expression of CD33 (23.6%, 38/161) compared to neardiploid/CD66c-positive (17.9%, 19/106) and hyperdiploid/CD66c-negative (4.6%, 2/44) cases. In CRLF2-positive/CD66c-positive cases, frequent expression of CD33 (36.4%, 4/11) but not CD13 was observed. Since positivity for CD15 and CD65 was low in BCP-ALL, with the exception of *MLL*-related chimeric gene-positive cases [18], no significant differences in the expression of these antigens depending on CD66c expression were observed (data not shown).

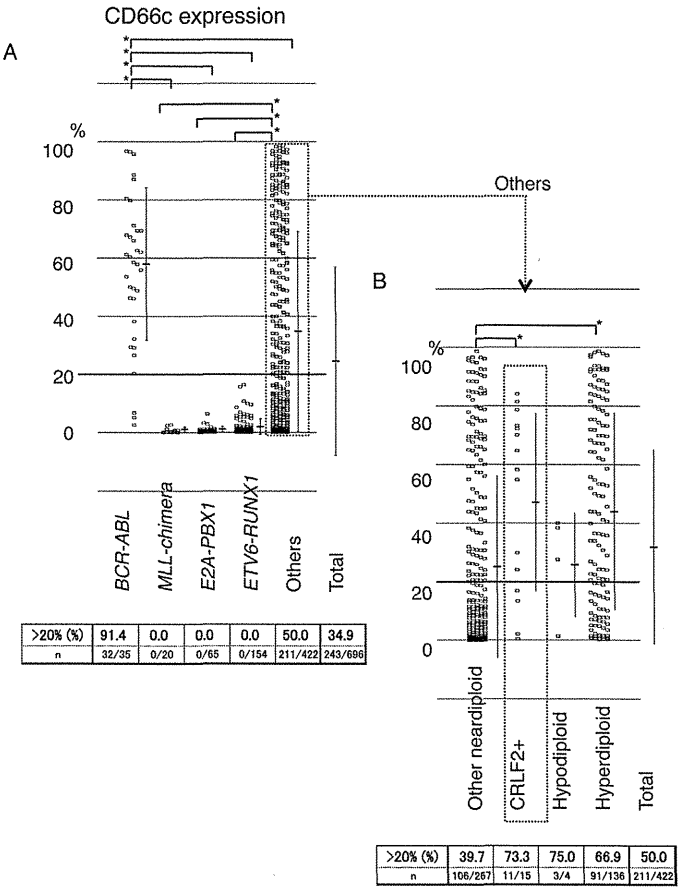

Fig. 1. Correlation between percentage CD66c positivity and acute lymphoblastic leukemia (ALL) genotype categories. (A) CD66c positivity (percentage) of B-cell precursor ALL ($n = 696$) was plotted on a scattergram categorized by the presence of well-known chimeric genes. Percentage of CD66c-positive cases (more than 20% expression in blasts) in each genotype group is listed below. (B) CD66c positivity (percentage) of B-cell precursor ALL without chimeric genes listed above ($n = 422$) was further subclassified based on the DNA-ploidy and CRLF2 expression and presented as in (A). *$p < 0.01$, using Student's t-test.

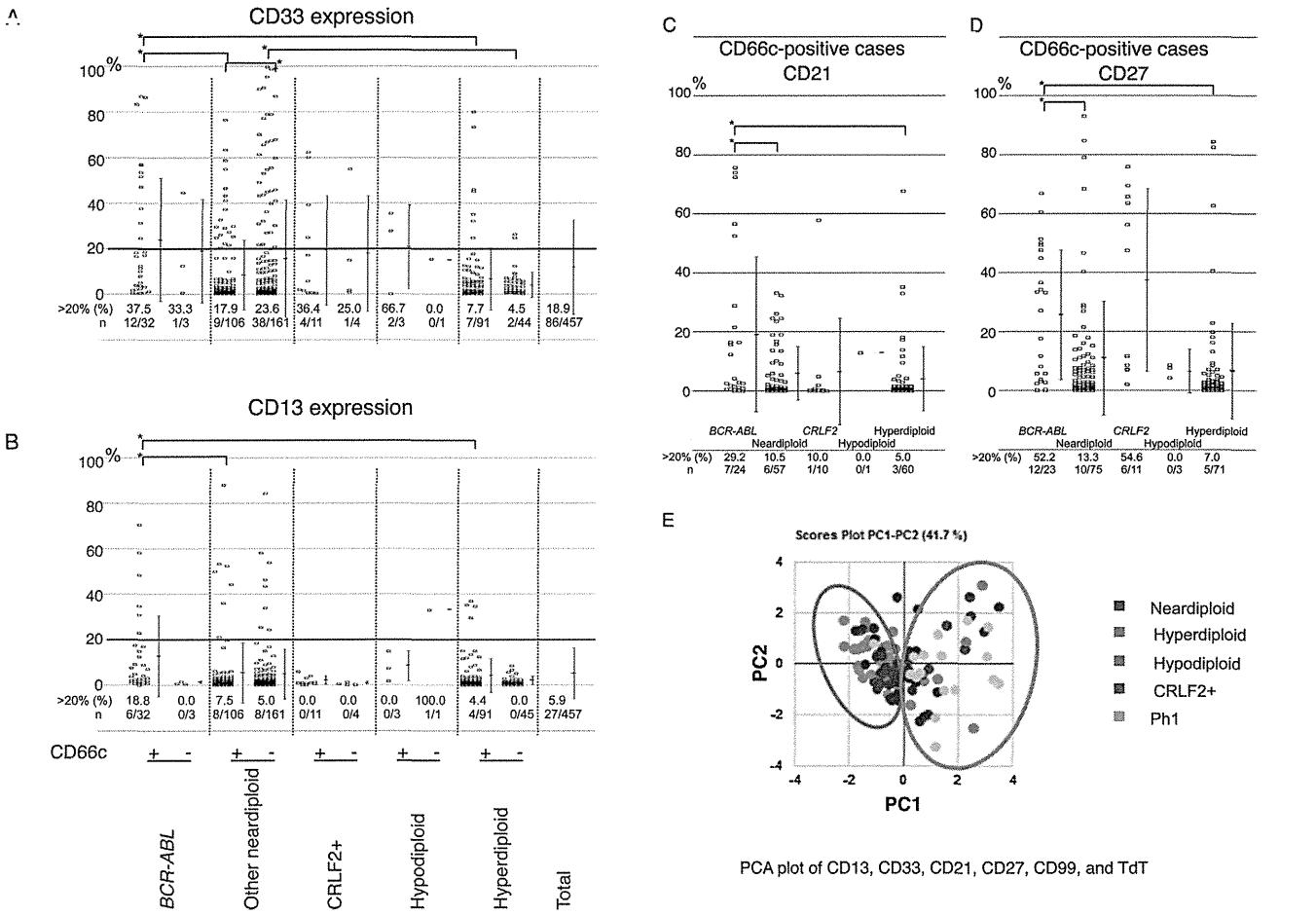

Fig. 2. Correlation between CD66c positivity and the expression of myeloid antigens, CD21 and CD27 in different genotype categories of acute lymphoblastic leukemia (ALL). The positivity (percentage) of CD33 (A) and CD13 (B) of B-cell precursor ALL was plotted on a scattergram categorized by the CD66c expression and genotype, as in Fig. 1. The positivity (percentage) of CD21 (C) and CD27 (D) of CD66c-positive B-cell precursor ALL was plotted on a scattergram categorized by the genotype as indicated in the figure. The percentage of positive cases (more than 20% expression in blasts) in each group is listed below. *$p < 0.01$, using Student's *t*-test. (E) Principal components analysis (PCA) was performed on CD66c-positive B-cell precursor ALL cases. PCA plot of 6 antigen expression, including CD13, CD33, CD21, CD27, CD99, and TdT, is presented with two PCA axes (PC1 vs PC2).

In an attempt to explore immunophenotypic characteristics distinguishing *BCR-ABL*-positive ALLs and other CD66c-positive ALLs, we observed relatively high expression of CD21 and CD27 in *BCR-ABL*-positive ALLs. The molecule CD21 is a mature B-cell antigen and its expression in BCP-ALL is very limited [19]. The CD27 molecule is a member of the TNF receptor family and known as a marker of mature memory B cells, while some malignant and nonmalignant B precursors also express this antigen [20]. Among CD66c-positive cases, CD21 expression was revealed to be relatively high in *BCR-ABL*-positive cases (Fig. 2C), and CD27 expression was high in both *BCR-ABL*-positive and CRLF2-overexpressing cases (Fig. 2D).

To further assess the biological relevance of the expression of above antigens in CD66c-positive ALL, we performed multivariate analyses by employing PCA. As shown in Fig. 2E, PCA plot using the expression data of 6 antigens, including CD13, CD33, CD21, CD27, CD99, and TdT, could roughly separate BCR-ABL-positive and CRLF2-positive cases from remaining chimeric gene-negative cases expressing CD66c.

3.4. Correlation between risk factors and CD66c expression

We next examined the correlation between CD66c expression and risk classification in chimeric gene-negative cases. In our protocol, the patients were stratified into three risk groups, namely, standard risk (SR), intermediate risk (IR), and high risk (HR), based on presenting features (age and the leukocyte count before starting the treatment) and, then, reclassified into them three categories 7 days later according to the sensitivity to oral prednisolone monotherapy, using the cut-off counts of 1000 blasts/μL [21]. As shown in Table 3, hyperdiploidy/CD66c-positive cases were more frequently classified into SR at diagnosis, while no difference was observed at reclassification on Day 8, indicating that hyperdiploid/CD66c-positive cases tend to have favorable initial presenting features but exhibit poor response for steroid. On the other hand, neardiploid/CD66c-negative cases tended to be more frequently classified into IR and HR at the initial classification, and the tendency appeared to be more significant at reclassification on Day 8 (Table 3), indicating that neardiploid/CD66c-negative have unfavorable presenting features as well as poor steroid sensitivity. After 5-year observation, however, no significant difference in the subsequent prognosis between CD66c-positive and -negative groups was observed (data not shown).

4. Discussion

Upon precisely analyzing CD66c expression in a large cohort of childhood BCP-ALL, we further extended the previous findings, and clearly identified the characteristics of CD66c expression as follows: First, among BCP-ALL possessing well-known chimeric genes, CD66c expression is highly selective in *BCR-ABL*-positive

Table 3
Risk classification and CD66c expression.

Hyper/	HR		IR		SR			Total	HR+IR/SR	
	(Case no.)								(Ratio)	
CD66c+	1		12		27			40	0.48	Initial
	HR-SCT	HR	HR	IR	HR	IR	SR			
	0	1	4	8	7	0	20		1.00	Day-8
Hyper/	HR		IR		SR					
CD66c-	0		8		8			16	1.00	Initial
	HR-SCT	HR	HR	IR	HR	IR	SR			
	0	0	1	7	0	0	8		1.00	Day-8
Diploid/	HR		IR		SR					
CD66c+	7		24		30			61	1.03	Initial
	HR-SCT	HR	HR	IR	HR	IR	SR			
	4	3	2	22	0	0	30		1.03	Day-8
Diploid/	HR		IR		SR					
CD66c-	14		48		31			93	2.00	Initial
	HR-SCT	HR	HR	IR	HR	IR	SR			
	8	6	4	44	3	0	28		2.32	Day-8

Hyper, hyperdiploid; Diploid, neardiploid; HR, high risk; IR, intermediate risk; SR, standard risk; SCT, stem-cell transplantation; Initial, risk classification based on presenting features; Day-8, re-risk classification after 7-day oral prednisolone monotherapy.

cases, while CD66c is never expressed in cases possessing not only *ETV6-RUNX1* and *MLL-AF4*, but also *MLL-AF9*, *MLL-ENL*, and *E2A-PBX1*. Second, among BCP-ALL cases without well-known chimeric genes, CD66c expression also exhibits some selectivity that correlates with genetic abnormalities and CRLF2-positive and probably hypodiploid states, and, as in hyperdiploidy cases tend to express CD66c at a high frequency. The results were schematically summarized in Fig. 3A. Above data indicate that CD66c expression has a close correlation with definite set of genetic abnormalities, although it is not limited to a specific one.

The overexpression of *CRLF2* arises from a translocation juxtaposing *CRLF2* to the *IGH* enhancer or an interstitial deletion (*CRLF2-P2RY8*) and has been reported to be found in 4.7% to 17.5% of BCP-ALL cases as assessed by real-time PCR [22–29]. In this study, however, we found only 15 CRLF2-positive cases (2.2%) in our cohort by flow cytometry. Although the precise reason for the inconsistency in the frequency of CRLF2 overexpression between previous reports by real-time PCR and our data of flow cytometry is remaining unclear, it is possibly due to the difference of detection methods including diagnostic criteria for positive case.

Most recently, a subtype of BCP-ALL including CRLF2-overexpressing cases has been called "Ph-like ALL" and identified to be sharing a transcriptional signature that significantly overlaps with a *BCR-ABL*-positive ALL and accompanied by high rates of relapse and poor overall survival [30]. Besides CRLF2-overexpressing cases, our preliminary results indicate that other Ph-like ALL cases also tend to frequently express CD66c (data not shown).

As well as CRLF2 overexpression [22–29], both *BCR-ABL*-positive [13,31] and hypodiploid patients are well known to show a poor prognosis [13–15]. In contrast, hyperdiploid BCP-ALL patients are generally accompanied by a relatively favorable therapeutic outcome [12,13]. Therefore, the expression of CD66c itself is not directly linked to the prognosis, whereas the genetic abnormalities accompanying CD66c expression are important to make a prognosis for BCP-ALL patients. Concerning the chimeric gene-negative cases, our data further indicated that the combination of CD66c expression and chromosome number abnormalities is closely related to risk classification and steroid sensitivity. Thus the genetic findings must be paid attention when CD66c expression is detected.

Since *CRLF2*-overexpressing BCP-ALLs and *BCR-ABL*-positive cases share overlaped transcriptional signature as we described above [24], the transcription of CD66c might be regulated by a common downstream factor in both pathways. Similarly, CD66c expression in hyper- and hypodiploid cases might also share the same pathway, whereas the precise mechanism that induces the aberrant expression of CD66c in BCP-ALL is unclear. In the

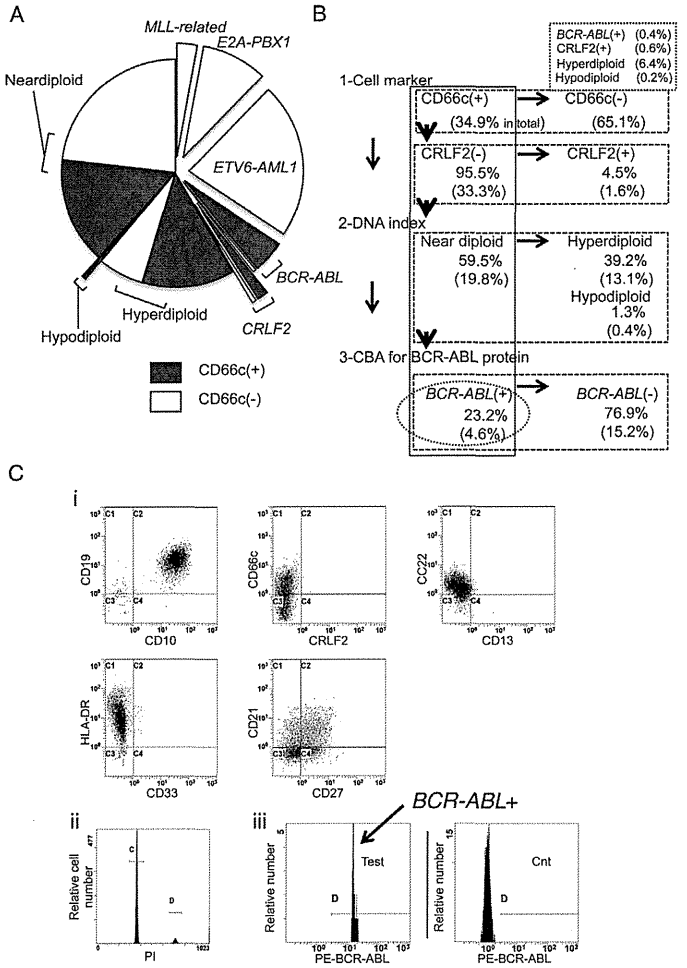

Fig. 3. Summary of CD66c expression and diagnostic flow to detect BCR-ABL-positive acute lymphoblastic leukemia (ALL) by flow cytometry. (A) Summary of CD66c expression and correlation with genetic abnormalities. (B) An initial diagnostic flow of the subclassification of BCP-ALL using flow cytometry is indicated. In the case of neardiploid B-cell precursor ALL that is CD66c-positive and CRLF2-negative, it is recommended to perform the Cytometric Bead Array (CBA) for BCR-ABL protein. Cases expressing any of the myeloid antigens, CD21, or CD27 and exhibiting extreme elevation of peripheral blood white blood cell counts are highly probable of being BCR-ABL-positive. The frequency (%) of each subclass in our study is indicated as a percentage. The number in parentheses indicates the frequency in the total cases. (C) Case diagnosed as BCR-ABL-positive ALL by flow cytometry. The leukemic cells exhibit CD19+, CD10+, HLA-DR+, CD22+, CD66c+, CRLF2-, myeloid-antigen-, CD21+, and CD27+. The DNA-index analysis revealed neardiploidy, and CBA for BCR-ABL protein was positive.

case of hyperdiploid ALLs, a significant correlation between the chromosomal location of upregulated genes and the presence of trisomies/tetrasomies was observed, and, thus, the reflection of a gene-dosage effect has been suggested [32]. On the other hand, hyperdiploid ALL is characterized by a nonrandom gain of chromosomes commonly including chromosomes X, 4, 6, 10, 14, 17, 18, and 21, but CD66c is located on chromosome 19 [33]. Considering the findings, the expression of CD66c in hyperdiploid cases should not be mediated by the gene-dosage effect.

It was reported that the expression of CD13, CD33, CD15, and CD65 tended to be mutually exclusive with CD66c [6]. Since both *ETV6-RUNX1*-positive ALL frequently expressing CD33 and CD13 [17] and ALL with *MLL*-related chimeric genes commonly expressing CD15 and CD65 [18] are highly concentrated in neardiploid/CD66c-negative cases, it is quite reasonable that the expressions of CD66c and other myeloid antigens tend to be mutually exclusive. Therefore, we excluded BCP-ALL cases possessing well-known chimeric genes lacking CD66c expression and then analyzed the correlation between CD66c expression and that of other myeloid antigens. However, upon excluding *ETV6-RUNX1*-positive cases from the analysis, neardiploid/CD66c-negative cases still exhibited a significantly higher expression of CD33. On the other hand, both *BCR-ABL*-positive and CRLF2-expressing cases exhibited frequent expression of CD33 besides CD66c. Further investigation of the underlying mechanisms that induce the aberrant expression of CD66c and other myeloid antigens should be conducted in the future.

Based on our analysis, we propose an initial diagnostic flow of the prognosis-based subclassification of BCP-ALL using flow cytometry. As presented in Fig. 3B and C, in addition to a regular diagnostic panel, the immunocytological detection of CD66c and CRLF2 in combination with PI staining should be a useful tool for the initial diagnosis of BCP-ALL. By assessing cases with PI staining, more than one-third of the patients should be diagnosed as hyperdiploid, and hypodiploid cases might be rarely detected. After the exclusion of hyper- and hypodiploid BCP-ALL cases, less than 10% of the cases will be CRLF2-positive. In the remaining cases, approximately one quarter of the cases should be *BCR-ABL*-positive ALL. As we presented in Fig. 2E by PCA, the coexpression of myeloid antigens, CD21 or CD27 with CD66c, as well as extreme elevation of peripheral blood white blood cell counts, suggests the presence of a *BCR-ABL* chimeric gene at a high probability, while the findings are not definitive. However, by utilizing the recently developed CBA for BCR-ABL protein, we can make a final diagnosis of *BCR-Abl*-positive ALL at the initial presentation of the patient without waiting for the results of RT-PCR or chromosomal analysis. Since the effectiveness of tyrosine kinase inhibitors as first-line treatment has been reported [31,34], the prompt diagnosis of *BCR-ABL*-positive ALL is important. In our pilot study on 20 patients suspected of *BCR-ABL*-positive ALL, including 5 cases subsequently confirmed as true *BCR-ABL*-positive, the results showed a complete concordance between prior CBA for BCR-ABL fusion proteins and following real-time PCR for *BCR-ABL* chimeric genes (a typical result was presented in Fig. 3C).

In conclusion, CD66c expression is not always specific for *BCR-ABL*-positive ALL, whereas it is frequently associated with some genetic abnormalities, which are important for the prognosis. Although further analysis is needed to elucidate the underlying genetic characteristics as well as clinico-pathological features of CD66c-positive neardiploid BCP-ALL cases, our observations should shed light on the significance of CD66c expression in BCP-ALL.

Conflict of interest statement

The authors have no conflict of interest to declare with regards to this work.

Acknowledgments

The authors thank the members of the ALL Committee of the TCCSG: Kazutoshi Koike, Hiroaki Goto, Takashi Kanazawa, Tetsuya Mori, Wataru Oyama, Junya Fujimura, Daisuke Toyama, Masa-aki Shiohara, Yasushi Noguchi, Setsuo Ohta, Hiromasa Yabe, Daisuke Tomizawa, Motohiro Kato, Hiroyuki Takahashi, Keitaro Fukushima, Takashi Kaneko, Takahiro Ueda, Ryosuke Kajiwara, Shinji Mochizuki, Manabu Sotomatsu, and Chitose Ogawa. We also thank Kaori Itagaki for preparing and refining the data of patients. This work was supported by a grant from Children's Cancer Association of Japan, Health and Labour Sciences Research Grants (the 3rd-term comprehensive 10-year strategy for cancer control H22-011), the Grant of National Center for Child Health and Development (25-2), a Grant-in-Aid for Young Scientists (B)

(2479110), and the Advanced research for medical products Mining Programme of the National Institute of Biomedical Innovation (NIBIO, 10-41, -42, -43, -44, -45).

Contributions. NK designed the research study, performed research, analyzed data and wrote the paper. OT, KI, MM, DH, KK, HO, MK, HS, AM, TK, NT and KK performed the research. AK, JF, YH AO analyzed data. TK, AM and KS analyzed data and wrote the paper.

Appendix A. Supplementary data

Supplementary data associated with this article can be found, in the online version, at http://dx.doi.org/10.1016/j.leukres.2013.10.008.

References

[1] Greaves MF, Chan LC, Furley AJ, Watt SM, Molgaard HV. Lineage promiscuity in hemopoietic differentiation and leukemia. Blood 1986;67:1–11.
[2] Schmidt CA, Przybylski GK. What can we learn from leukemia as for the process of lineage commitment in hematopoiesis? Int Rev Immunol 2001;20:107–15.
[3] Béné MC, Porwit A. Acute leukemias of ambiguous lineage. Semin Diagn Pathol 2012;29:12–8.
[4] Sugita K, Mori T, Yokota S, Kuroki Ma, O-Koyama T, Inukai T, et al. The KOR-SA3544 antigen predominantly expressed on surface of Philadelphia chromosome-positive acute lymphoblastic cells is nonspecific cross-reacting antigen-50/90 (CD66c) and invariably expressed in cytoplasm of human leukemia cells. Leukemia 1999;13:779–85.
[5] Boccuni P, Di Noto R, Lo Pardo C, Villa MR, Ferrara F, Rotoli B, et al. CD66c antigen expression is myeloid restricted in normal bone marrow but is a common feature of CD10+ early-B-cell malignancies. Tissue Antigens 1998;52:1–8.
[6] Kalina T, Vaskova M, Mejstrikova E, Madzo J, Trka J, Stary J, et al. Myeloid antigens in childhood lymphoblastic leukemia: clinical data point to regulation of CD66c distinct from other myeloid antigens. BMC Cancer 2005;5:38.
[7] Mori T, Sugita K, Suzuki T, Okazaki T, Manabe A, Hosoya R, et al. A novel monoclonal antibody, KOR- SA3544 which reacts to Philadelphia chromosome-positive acute lymphoblastic leukemia cells with high sensitivity. Leukemia 1995;9:1233–9.
[8] Hrusák O, Trka J, Zuna J, Housková J, Bartůnková J, Starý J. Aberrant expression of KOR-SA3544 antigen in childhood acute lymphoblastic leukemia predicts TEL-AML1 negativity. The Pediatric Hematology Working Group in the Czech Republic. Leukemia 1998;12:1064–70.
[9] Yamanka T, Kuroki M, Matsuo Y, Matsuoka Y. Analysis of heterophilic cell adhesion mediated by CD66b and CD66c using their soluble recombinant proteins. Biochem Biophys Res Commun 1996;219:842–7.
[10] Klein ML, McGhee SA, Baranian J, Stevens L, Hefta SA. Role of non- specific cross-reacting antigen, a CD66 cluster antigen, in activation of human granulocytes. Infect Immun 1996;64:4574–9.
[11] Kanderová V, Hrusák O, Kalina T. Aberrantly expressed CEACAM6 is involved in the signaling leading to apoptosis of acute lymphoblastic leukemia cells. Exp Hematol 2010;38:653–60.
[12] Paulsson K, Johansson B. High hyperdiploid childhood acute lymphoblastic leukemia. Genes Chromosomes Cancer 2009;48:637–60.
[13] Pui CH, Mullighan CG, Evans WE, Relling MV. Pediatric acute lymphoblastic leukemia: where are we going and how do we get there? Blood 2012;120:1165–74.
[14] Harrison CJ, Moorman AV, Broadfield ZJ, Cheung KL, Harris RL, Reza Jalali G, et al. Childhood and Adult Leukaemia Working Parties. Three distinct subgroups of hypodiploidy in acute lymphoblastic leukaemia. Br J Haematol 2004;125:552–9.
[15] Nachman JB, Heerema NA, Sather H, Camitta B, Forestier E, Harrison CJ, et al. Outcome of treatment in children with hypodiploid acute lymphoblastic leukemia. Blood 2007;110:1112–5.
[16] Greipp PR, Trendle MC, Leong T, Oken MM, Kay NE, Van Ness B, et al. Is flow cytometric DNA content hypodiploidy prognostic in multiple myeloma? Leuk Lymphoma 1999;35:83–9.
[17] Baruchel A, Cayuela JM, Ballerini P, Landman-Parker J, Cezard V, Firat H, et al. The majority of myeloid-antigen-positive (My+) childhood B-cell precursor acute lymphoblastic leukaemias express TEL-AML1 fusion transcripts. Br J Haematol 1997;99:101–6.
[18] Behm FG, Smith FO, Raimondi SC, Pui CH, Bernstein ID. Human homologue of the rat chondroitin sulfate proteoglycan, NG2, detected by monoclonal antibody 7.1, identifies childhood acute lymphoblastic leukemias with t(4;11)(q21;q23) or t(11;19)(q23;p13) and MLL gene rearrangements. Blood 1996;87:1134–9.
[19] Uckun FM. Regulation of human B-cell ontogeny. Blood 1990;76:1908–23.
[20] Vaskova M, Fronkova E, Starkova J, Kalina T, Mejstrikova E, Hrusak O. CD44 and CD27 delineate B-precursor stages with different recombination status and with an uneven distribution in nonmalignant and malignant hematopoiesis. Tissue Antigens 2008;71:57–66.
[21] Manabe A, Ohara A, Hasegawa D, Koh K, Saito T, Kiyokawa N, et al. Significance of the complete clearance of peripheral blasts after 7 days of prednisolone treatment in children with acute lymphoblastic leukemia: the Tokyo Children's Cancer Study Group Study L99-15. Haematologica 2008;93:1155–60.
[22] Mullighan CG, Collins-Underwood JR, Phillips LA, Loudin MG, Liu W, Zhang J, et al. Rearrangement of CRLF2 in B-progenitor- and Down syndrome-associated acute lymphoblastic leukemia. Nat Genet 2009;41:1243–6.
[23] Russell LJ, Capasso M, Vater I, Akasaka T, Bernard OA, Calasanz MJ, et al. Deregulated expression of cytokine receptor gene, CRLF2, is involved in lymphoid transformation in B-cell precursor acute lymphoblastic leukemia. Blood 2009;114:2688–98.
[24] Yoda A, Yoda Y, Chiaretti S, Bar-Natan M, Mani K, Rodig SJ, et al. Functional screening identifies CRLF2 in precursor B-cell acute lymphoblastic leukemia. Proc Natl Acad Sci USA 2010;107:252–7.
[25] Harvey RC, Mullighan CG, Chen IM, Wharton W, Mikhail FM, Carroll AJ, et al. Rearrangement of CRLF2 is associated with mutation of JAK kinases, alteration of IKZF1, Hispanic/Latino ethnicity, and a poor outcome in pediatric B-progenitor acute lymphoblastic leukemia. Blood 2010;115:5312–21.
[26] Cario G, Zimmermann M, Romey R, Gesk S, Vater I, Harbott J, et al. Presence of the P2RY8-CRLF2 rearrangement is associated with a poor prognosis in non-high-risk precursor B-cell acute lymphoblastic leukemia in children treated according to the ALL-BFM 2000 protocol. Blood 2010;115:5393–7.
[27] Ensor HM, Schwab C, Russell LJ, Richards SM, Morrison H, Masic D, et al. Demographic, clinical, and outcome features of children with acute lymphoblastic leukemia and CRLF2 deregulation: results from the MRC ALL97 clinical trial. Blood 2011;117:2129–36.
[28] Chen IM, Harvey RC, Mullighan CG, Gastier-Foster J, Wharton W, Kang H, et al. Outcome modeling with CRLF2, IKZF1, JAK, and minimal residual disease in pediatric acute lymphoblastic leukemia: a Children's Oncology Group study. Blood 2012;119:3512–22.
[29] Palmi C, Vendramini E, Silvestri D, Longinotti G, Frison D, Cario G, et al. Poor prognosis for P2RY8-CRLF2 fusion but not for CRLF2 over-expression in children with intermediate risk B-cell precursor acute lymphoblastic leukemia. Leukemia 2012;26:2245–53.
[30] Roberts KG, Morin RD, Zhang J, Hirst M, Zhao Y, Su X, et al. Genetic alterations activating kinase and cytokine receptor signaling in high-risk acute lymphoblastic leukemia. Cancer Cell 2012;22:153–66.
[31] Hunger SP. Tyrosine kinase inhibitor use in pediatric Philadelphia chromosome-positive acute lymphoblastic anemia. Hematology Am Soc Hematol Educ Program 2011;2011:361–5.
[32] Andersson A, Olofsson T, Lindgren D, Nilsson B, Ritz C, Edén P, et al. Molecular signatures in childhood acute leukemia and their correlations to expression patterns in normal hematopoietic subpopulations. Proc Natl Acad Sci USA 2005;102:19069–74.
[33] Inazawa J, Abe T, Inoue K, Misawa S, Oikawa S, Nakazato H, et al. Regional assignment of nonspecific cross-reacting antigen (NCA) of the CEA gene family to chromosome 19 at band q13.2. Cytogenet Cell Genet 1989;52:28–31.
[34] Foà R, Vitale A, Vignetti M, Meloni G, Guarini A, De Propris MS, et al. GIMEMA Acute Leukemia Working Party. Dasatinib as first-line treatment for adult patients with Philadelphia chromosome-positive acute lymphoblastic leukemia. Blood 2011;118:6521–8.

MYELOID NEOPLASIA

Clonal selection in xenografted TAM recapitulates the evolutionary process of myeloid leukemia in Down syndrome

Satoshi Saida,[1] Ken-ichiro Watanabe,[1] Aiko Sato-Otsubo,[2] Kiminori Terui,[3] Kenichi Yoshida,[2] Yusuke Okuno,[2] Tsutomu Toki,[3] RuNan Wang,[3] Yuichi Shiraishi,[4] Satoru Miyano,[4] Itaru Kato,[1] Tatsuya Morishima,[1] Hisanori Fujino,[1] Katsutsugu Umeda,[1] Hidefumi Hiramatsu,[1] Souichi Adachi,[5] Etsuro Ito,[3] Seishi Ogawa,[2] Mamoru Ito,[6] Tatsutoshi Nakahata,[7] and Toshio Heike[1]

[1]Department of Pediatrics, Graduate School of Medicine, Kyoto University, Kyoto, Japan; [2]Cancer Genomics Project, Graduate School of Medicine, University of Tokyo, Tokyo, Japan; [3]Department of Pediatrics, Graduate School of Medicine, Hirosaki University, Hirosaki, Japan; [4]Laboratory of DNA Information Analysis, Human Genome Center, Institute of Medical Science, University of Tokyo, Tokyo, Japan; [5]Department of Human Health Sciences, Graduate School of Medicine, Kyoto University, Kyoto, Japan; [6]Laboratory Animal Research Department, Central Institute for Experimental Animals, Kawasaki, Japan; and [7]Department of Clinical Application, Center for iPS Cell Research and Application, Kyoto University, Kyoto, Japan

Key Points

- Genetically heterogeneous subclones with varying leukemia-initiating potential exist in neonatal transient abnormal myelopoiesis.
- This novel xenograft model of transient abnormal myelopoiesis may provide unique insight into the evolutionary process of leukemia.

Transient abnormal myelopoiesis (TAM) is a clonal preleukemic disorder that progresses to myeloid leukemia of Down syndrome (ML-DS) through the accumulation of genetic alterations. To investigate the mechanism of leukemogenesis in this disorder, a xenograft model of TAM was established using NOD/Shi-*scid*, interleukin (IL)-2Rγ^{null} mice. Serial engraftment after transplantation of cells from a TAM patient who developed ML-DS a year later demonstrated their self-renewal capacity. A *GATA1* mutation and no copy number alterations (CNAs) were detected in the primary patient sample by conventional genomic sequencing and CNA profiling. However, in serial transplantations, engrafted TAM-derived cells showed the emergence of divergent subclones with another *GATA1* mutation and various CNAs, including a 16q deletion and 1q gain, which are clinically associated with ML-DS. Detailed genomic analysis identified minor subclones with a 16q deletion or this distinct *GATA1* mutation in the primary patient sample. These results suggest that genetically heterogeneous subclones with varying leukemia-initiating potential already exist in the neonatal TAM phase, and ML-DS may develop from a pool of such minor clones through clonal selection. Our xenograft model of TAM may provide unique insight into the evolutionary process of leukemia. (*Blood*. 2013;121(21):4377-4387)

Introduction

Neonates with Down syndrome (DS) are at high risk of developing a unique hematologic disorder referred to as transient abnormal myelopoiesis (TAM), transient myeloproliferative disorder, or transient leukemia. In most cases, TAM resolves spontaneously within 3 months.[1,2] However, after spontaneous remission, 20% of TAM patients develop myelodysplastic syndrome and acute megakaryocytic leukemia referred to as myeloid leukemia of DS (ML-DS) within 4 years.[3,4] Blast cells in most patients with TAM and ML-DS have mutations in exon 2 of the gene coding for the transcription factor *GATA1*,[5-8] which is essential for the normal development of erythroid and megakaryocytic cells.[9,10] Although blast cells in most TAM and ML-DS patients share the identical *GATA1* mutation, recurrent additional cytogenetic abnormalities are commonly observed during disease progression.[2,5,11,12] In fact, a ML-DS case derived from a minor clone with a distinct *GATA1* mutation in the TAM phase was previously reported by our group.[13] These clinical findings suggest that although most TAM cells disappear in the early neonatal phase, a few clones persist during apparent remission to develop ML-DS later. Because only one fifth of TAM cases progress to ML-DS, additional genetic events besides *GATA1* mutation are likely to be involved in the progression of TAM to ML-DS.[14] As mentioned above, the development of ML-DS is significantly correlated with karyotypic abnormalities such as duplication (dup)(1q), deletion (del)(6q), del(7p), dup(7q), +8, +11, and del(16q),[2,11,12] which are rarely observed in the TAM phase. These clinical findings have led many physicians to consider TAM as preleukemia and the progression of TAM to ML-DS as an attractive model to investigate multistep leukemogenesis.

Animal models have contributed to our understanding of the pathogenesis of TAM/ML-DS and other leukemias.[15-21] Mice models in which primary human leukemic cells were transplanted into immunodeficient hosts provided significant clues to advance our understanding of the pathogenesis of human leukemia.[19-22] However,

Submitted December 18, 2012; accepted February 4, 2013. Prepublished online as *Blood* First Edition paper, March 12, 2013; DOI 10.1182/blood-2012-12-474387.

The online version of this article contains a data supplement.

The publication costs of this article were defrayed in part by page charge payment. Therefore, and solely to indicate this fact, this article is hereby marked "advertisement" in accordance with 18 USC section 1734.

xenograft models of primary patient samples from the preleukemic phase have been rarely reported, and the TAM xenograft model would be an attractive method to investigate leukemogenesis.

We previously described the development of novel immunodeficient NOD/Shi-*scid*, interleukin (IL)-2Rγ^{null} (NOG) mice with a superior capacity for the engraftment of human hematopoietic and neoplastic cells.[23-26] In contrast to a previous study in which TAM cells showed a limited ability to expand in immunodeficient mice,[27] we established a xenograft model where TAM cells were transplanted into NOG mice to recapitulate the pathophysiology of TAM/ML-DS. This xenograft model in combination with high-throughput genomic technology was used to show that genetically heterogeneous minor subclones with leukemia-initiating potential already exist in the neonatal TAM phase and could serve as initiating clones evolving to ML-DS in a patient. Our TAM xenograft model may be of value to gain insight into the evolutionary process of leukemia.

Materials and methods

Patients and sample collection

Peripheral blood (PB) samples were obtained from patients diagnosed with TAM associated with DS in acute and complete remission phases. Mononuclear cells were separated by Ficoll-Hypaque (Pharmacia, Uppsala, Sweden) density gradient centrifugation, as previously described.[23] Informed consent was obtained from the patients' parents in accordance with the Declaration of Helsinki, and the research was approved by the institutional ethics committee of Kyoto University Hospital.

Mice

NOG mice were developed at the Central Institute of Experimental Animals (Kawasaki, Japan) as previously described[28] and were maintained in our pathogen-free facility and cared for in accordance with the institutional guidelines for animal welfare.

Primary and serial xenogeneic transplantation into NOG mice

Xenotransplantation and analysis of TAM cells were performed using a previously reported method with some modifications.[26] In brief, PB mononuclear cells (PBMCs) obtained from TAM patients (1–3 $\times$ 10^6 cells) were injected into 2.4 Gy–irradiated 8- to 12-week-old NOG mice through the tail vein. To screen for the proliferation of TAM-derived cells, bone marrow (BM) cells were aspirated from the tibia every 4 weeks. Engraftment was defined as >1% of cells staining positive for human CD7 (hCD7), hCD33, hCD41a, hCD45, and hCD117 at 12 weeks after transplantation. For serial transplantation, recipient BM cells were collected 12 to 18 weeks after transplantation; the equivalent of 1 $\times$ 10^6 hCD45$^+$ cells was intravenously transplanted into new mice. For a detailed determination of chromosomal and genetic alterations in TAM-derived cells, serial transplantation experiments using preserved PBMC samples were performed.

Flow cytometric analysis of transplanted TAM-derived cells

For analysis of TAM-derived cells in murine BM, mice were euthanized, and the BM was removed and mechanically dispersed. Mononuclear cells were purified from the BM and stained with antibodies. Dead cells were excluded according to 4′,6-diamidino-2-phenylindole staining. Blast cells were identified by classical CD45/SSC blast gating.[29] See supplemental Methods on the *Blood* Web site for details.

Human cell sorting

Human cell isolation was performed according to a previously described method with some modifications.[23,24] See supplemental Methods for details.

Colony assay

Leukemic colony formation was assessed according to a previously described method with some modifications.[30] See supplemental Methods for details.

GATA1 genomic sequencing analysis

The *GATA1* gene was amplified using polymerase chain reaction (PCR) as previously described[8] and sequenced by an ABI 3130xl Genetic analyzer (Applied Biosystems, Foster City, CA).

DNA copy number analysis

DNA copy number analysis was performed using GeneChip Human Mapping 250K Nsp arrays (Affymetrix, Inc., Santa Clara, CA) according to the manufacturer's standard protocols. Genomic copy numbers including allele-specific copy numbers were calculated using CNAG/AsCNAR software (http://www.genome.umin.jp), and genomic DNA obtained from PB of patients in the remission phase was used as a control. Copy number abnormalities and other allelic imbalances were detected using a hidden Marcov model–based algorithm.

Statistical analysis

Data are presented as the mean ± standard deviation. The 2-sided P value was determined by testing the null hypothesis that the 2 population medians are equal. P values <0.05 were considered to be significant.

Results

Establishment of a TAM xenograft model using NOG mice

To determine whether NOG mice provide a TAM xenograft model, Ficoll-purified PB samples from 11 TAM patients were transplanted into irradiated NOG mice. Patient characteristics are shown in Table 1. Patients' ages at sample collection, percentage of blast cells, number of cells injected, and number of engrafted recipients for each PB sample are shown in supplemental Table 1. Of 11 patient samples, 3 (patients 1, 2, and 9) were engrafted successfully in the recipient mice. Engraftment was maintained ⩾12 weeks in all cases (Figure 1A). The spleen and liver of the recipients were also infiltrated with hCD45$^+$ blast cells (data not shown). These TAM-derived cells were morphologically similar to the primary TAM cells obtained from the patients (Figure 1B). Flow cytometric analysis of surface antigens detected the expression of CD117, CD34, CD33, and CD41a on hCD45$^+$ cells, which was consistent with the pattern observed in primary cells of TAM patients (Figure 1C). The presence of the same *GATA1* mutation was confirmed in the primary TAM cells and the engrafted cells in NOG mice (Figure 1D; supplemental Table 1). Chromosomal analysis of engrafted cells showed no abnormalities other than trisomy 21 (Figure 1E). These TAM-derived cells were detectable in the recipient's BM for >24 weeks (data not shown).

NOG mice can support self-renewal of TAM-derived cells

To examine the self-renewal capacity of TAM-derived cells, we performed serial transplantation of engrafted cells in the BM of recipient mice. Only the TAM-derived cells from patient 1 were successfully engrafted into the secondary (2°) and tertiary (3°) recipients. The morphology and surface antigen expression of these engrafted cells remained unchanged throughout the serial transplantation (Figure 2A-B). Interestingly, the TAM-derived cells

Table 1. Clinical characteristics of 11 TAM patients

Patient no.	Gender	Period of gestation, wk	Weight at birth, g	PB at diagnosis of TAM				Cytogenetics International System for Human Cytogenetic Nomenclature (2009)	*GATA1* mutation	Treatment		Clinical outcome	Onset of ML-DS (m of age)	Follow-up interval
				WBC, $\times 10^3$/μL	Blast, %	Hb, g/dL	Plt, $\times 10^3$/μL			Exchange transfusion	Low-dose Ara-C			
1	F	36	3050	159	91	9.1	247	47,XX,+21 [20]	c.38_39delAG	No	Yes	Alive	Yes (14)	27
2	M	37	1868	45.0	65	19.0	80	47,XY,+21 [20]	c.49C>T	No	Yes	Alive	No	24
3	F	39	3102	40.3	37	15.1	304	47,XX,+21 [20]	c.59_174del116	No	No	Alive	No	23
4	M	37	2780	15.6	24	17.0	50	47,XY,+21 [20]	c.163_169del	No	No	Alive	No	22
5	M	39	3052	60.9	48	20.7	258	47,XY,+21 [19]	c.37G>T	No	No	Alive	No	21
6	F	37	2050	13.6	12	20.9	291	47,XX,+21 [20]	N/A	No	No	Alive	No	19
7	M	38	2694	280	87	13.6	26	47,XY,+21 [20]	c.186C>G	Yes	Yes	DOD	No	1
8	M	35	2070	174	80	19.2	117	47,XY,+21 [20]	c.-19-1G>A, c.1A>G	Yes	No	Alive	No	17
9	M	39	3380	56.2	65	20.2	156	47,XY,+21 [20]	c.35C>G	No	Yes	Alive	No	14
10	M	36	2131	199	84	12.2	73	47,XY,+21 [20]	c.19_20insCCTGA	Yes	Yes	Alive	No	14
11	F	33	2032	254	90	14.3	178	47,XX,+21 [20]	c.-19-62_-5delinsA	Yes	Yes	Alive	No	10

Brackets under International System for Human Cytogenetic Nomenclature indicate the number of analyzed cells in metaphase.
Ara-C, cytosine arabinoside; DOD, died of disease; Hb, hemoglobin; N/A, not assessed; Plt, platelet; WBC, white blood cell.

expanded rapidly in the 3° recipients (Figure 2C). The colony-forming ability of the engrafted cells also increased in subsequent generations (Figure 2D). These cells could be grown by serial transplantation for >1 year and ⩾8° recipients, indicating that some TAM clones had long-term self-renewal capacity, a characteristic of leukemia. Indeed, patient 1 developed ML-DS at the age of 1 year, whereas the other patients did not (Table 1).

TAM-NOG xenograft model recapitulates leukemic evolution from TAM

Additional chromosomal alterations are frequently observed in ML-DS in comparison with TAM, suggesting that these alterations in genomic structure could be related to the evolution of ML-DS from TAM.[2,11,12] Therefore, we first investigated whether the serially engrafted TAM-derived cells (from patient 1) had DNA copy number alterations (CNAs) using Affymetrix GeneChip Mapping 250K arrays. Primary samples from patient 1 had no CNAs other than the gain of chromosome 21. However, the TAM-derived cells in the 1° recipients showed heterozygous deletion of 16q22 and 16q24 (Figure 3). To determine whether these deletions were present in the same cell, we calculated the signal intensities of each deletion using array data. Nearly 100% of TAM-derived cells harbored each deletion, indicating that these 2 deletions exist in a single TAM-derived cell. Although 2° recipients showed the same CNAs, 3° recipients showed additional CNAs, namely the gain of the entire chromosome 1q (Figure 3; supplemental Figure 1A). Interestingly, the 1q gain was not detected in the 4° to 7° recipients, whereas deletions of 16q22 and 16q24 were present (Figure 3). In this series of transplantations, the original *GATA1* mutation found in the primary patient sample (patient 1) remained unchanged (supplemental Figure 1B).

Gain of 1q and deletions in 16q are recurrent chromosomal abnormalities in ML-DS.[11,12,31] The result of G-band karyotyping of TAM-derived cells in 3° recipients was 47,XX,+1, der (1;15)(q10;q10),+21 in 20/20 metaphase cells (supplemental Figure 1C), confirming genomic structural change, which is a hallmark of ML-DS. These data suggest that leukemic evolution of TAM-derived cells was observed in our NOG mouse model.

Genetically heterogeneous subclones with varying repopulating capacity expanded in the TAM-NOG xenograft model

To examine the kinetics of the leukemic evolution of TAM cells, another 2 sets of serial transplantations were performed using the preserved patient 1 sample (Figure 4A). Four of 5 mice in the second group (m2-1–m2-5) and 5 of 11 mice in the third group (m3-1–m3-11) harbored TAM cells from the patient. Of the total of 9 engrafted mice, 2 had the same CNAs detected in the first series of serial transplantations: deletion of 16q22 and 16q24 (m3-5 and m3-8; Figure 3). Moreover, 2 combinations of new CNAs were detected in the 1° recipients: deletion of 9q22 +12p12 (m3-4 and m3-7) and gain of 1q25.2-1q44 (m3-11). No CNAs other than the gain of chromosome 21 were detected in the other recipients (m2-1, m2-2, m2-4, and m2-5).

Each 1° engrafted mouse was subjected to 2° transplantation, and 5 of 9 series (m2-5, m3-4, m3-7, m3-8, and m3-11) successfully gave rise to the xenografts in the 2° recipients. It is noteworthy that the TAM-derived cells of the 2° recipients in 2 of the 3 analyzed series (m2-5 and m3-4) acquired additional CNAs, whereas the CNAs in 2 descendent 2° recipients of m3-8 remained unchanged. The additional CNA of gain of 1q was detected in the 2° recipients of m3-4, similar to that observed in the 3° recipient in Figure 3. Although

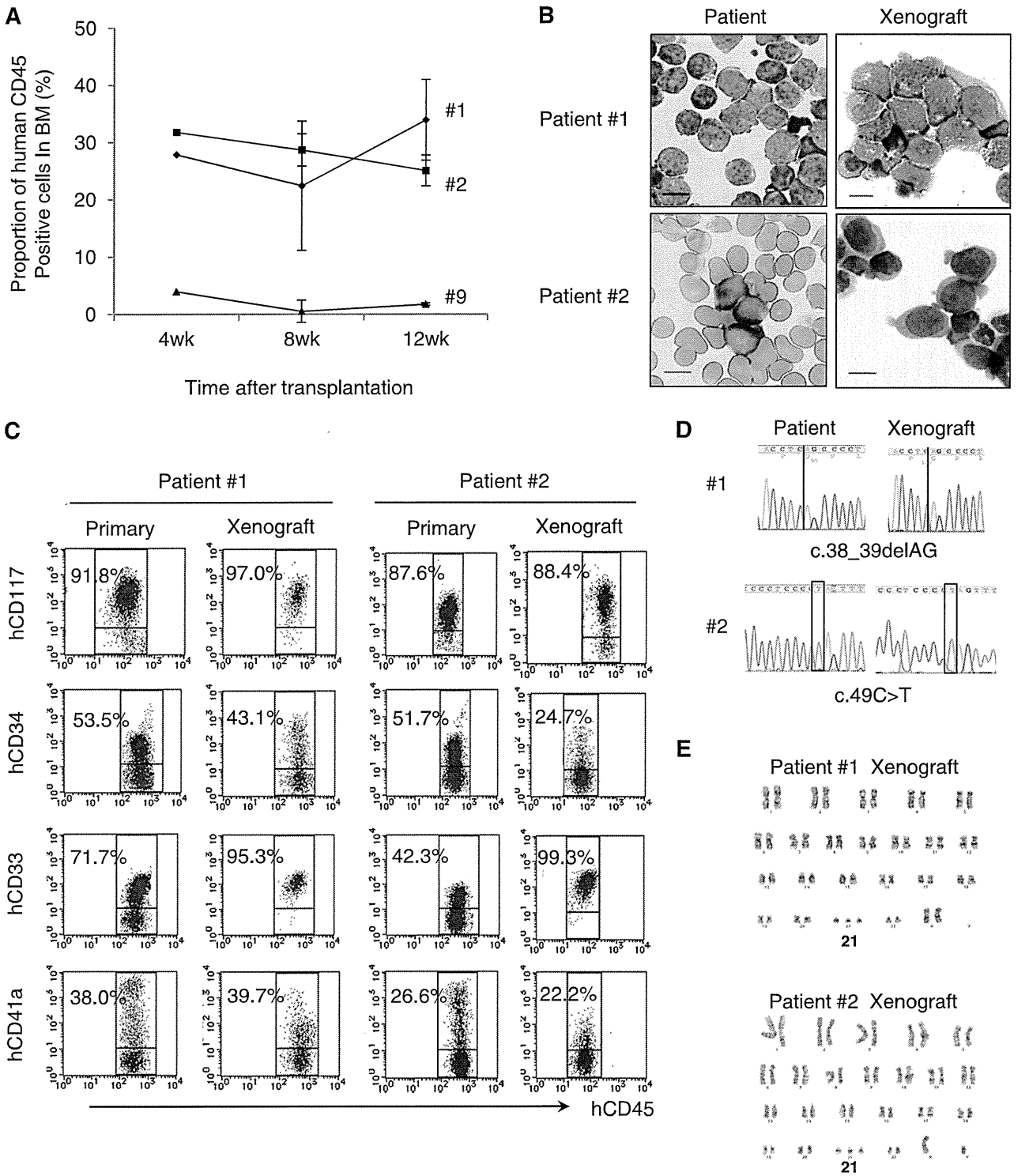

Figure 1. TAM cells engrafted in NOG mice. (A) Proportion of human CD45$^+$ cells in the BM of NOG mice at 4, 8, and 12 weeks after transplantation (n = 3–5 per group). (B) May-Giemsa staining of the BM smear of patients and cytospin preparation of human CD45$^+$ cells in the recipient NOG mice. Blast cells with cytoplasmic blebbing consistent with megakaryocytic differentiation were present in the BM of recipient mice. (C) Surface marker analysis of engrafted TAM cells. Human CD45$^+$ TAM-derived cells expressing hCD117, hCD34, hCD33, and hCD41a are detected in the recipient's BM. Blast cells were identified by CD45/SSC gating, and debris (low forward scatter) and dead cells (4′,6-diamidino-2-phenylindole positive) were excluded from the analysis. A representative result of >3 experiments is shown. (D) Genomic direct sequencing shows the presence of concordant GATA1 mutation in xenograft and original patients (1 and 2). (E) G-band karyotyping of TAM-derived cells in recipient murine BM shows no additional chromosome abnormality apart from constitutional trisomy 21, consistent with the findings in the original patients. The GATA1 mutation and the karyotype of engrafted cells from patient 9 were not assessed because of a low cell number.

gain of 1q was recurrently observed in this series, the duplicated regions were diverse: 1q25.2-1q44 (1°, m3-11), 1q21.3-1q44 (2°, m3-4), 1q31.2-1q44 (2°, m3-4), and the whole arm of chromosome 1q (3° in Figures 3 and 4A; supplemental Figure 2). In m2-5, a deletion of 3q24 appeared in the 2° and 3° recipients. These results demonstrated that TAM cells derived from patient 1

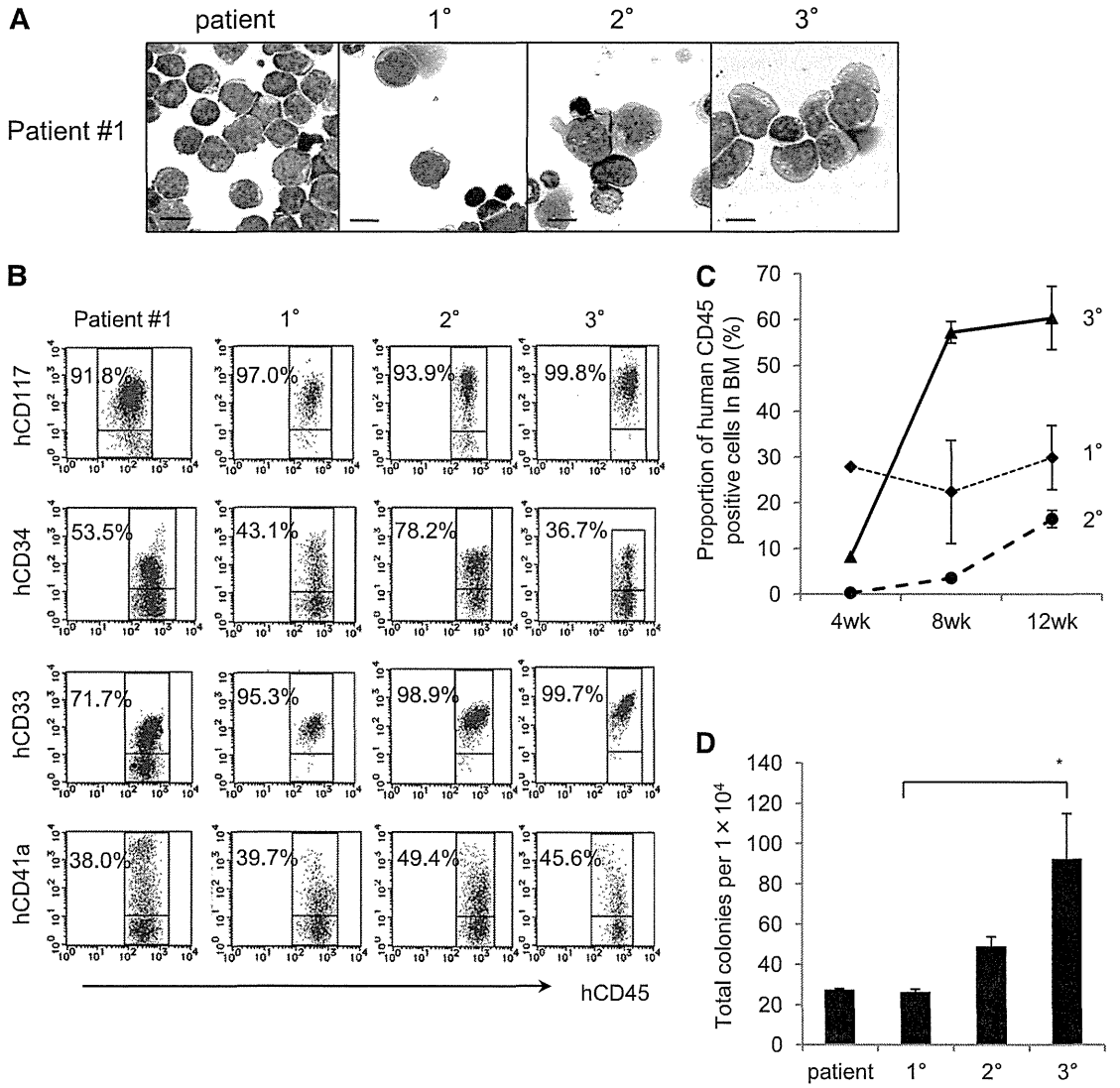

Figure 2. The NOG mouse model can support self-renewal of TAM-derived cells. (A) May-Giemsa staining of TAM-derived cells in recipients of patient 1. (B) Surface marker analysis of TAM-derived cells in recipients by flow cytometry. Viable cells were gated according to their forward scatter (FSC) and 4′,6-diamidino-2-phenylindole staining, blast cells were identified by CD45/SSC gating, and hCD45$^+$-gated cells were tested for the expression of hCD117, hCD34, hCD33, and hCD41a. (C) Proportion of hCD45$^+$ cells in BM of 1°, 2°, and 3° recipient mice at 4, 8, and 12 weeks after transplantation. (D) Colony assay of hCD45$^+$ cells in BM of 1°, 2°, and 3° recipient mice. hCD45$^+$ cells were seeded at 1.0×10^4 cells per 35-mm dish in triplicate, and the number of colonies in each dish was counted. Bars represent the standard deviation of the mean of 3 independent experiments. *Significant difference ($P < .05$).

acquired various CNAs and showed divergent repopulating capacity in our xenograft model.

TAM-NOG xenograft model revealed the presence of a minor clone with a distinct GATA1 mutation

ML-DS can arise from a minor TAM clone with a *GATA1* mutation that is distinct from that of the major TAM clone in a patient.[13] To determine whether the *GATA1* mutation in the primary patient's TAM cells was preserved in engrafted TAM-derived cells, *GATA1* mutation analysis was performed. TAM-derived cells in the series m3-4, m3-5, m3-7, and m3-8 had the same *GATA1* mutation (c.38_39delAG) as that of patient 1 (Figure 4A). Surprisingly, this mutation was not detected in TAM-derived cells in m2-1, m2-2, m2-5, and m3-11; instead, these samples showed a distinct *GATA1* mutation (c.1A>G) that was not detectable in the primary patient sample by direct sequencing. One of the 1° recipients (m2-4) showed both *GATA1* mutations. These results suggested that a minor clone with a distinct *GATA1* mutation (c.1A>G) was present in the primary patient sample and that this minor clone coexisted with, or predominated over, other clones in some 1° recipients. Therefore, a mutation-specific restriction enzyme digestion assay was performed using the primary sample from patient 1, which confirmed the presence of cells with the *GATA1* mutation (c.1A>G) as a minor clone (Figure 4B). Moreover, this minor clone propagated and acquired CNAs in NOG mice independently of the major clones (Figure 4A), further demonstrating the genetic heterogeneity of TAM cells. Interestingly, the major clone in the original patient 1 sample with a c.38_39delAG *GATA1* mutation and no CNAs did not become dominant in any of the recipients.

Minor subclone with additional CNAs was present in the primary TAM patient sample

TAM-derived cells in multiple 1° recipients derived from patient 1 had various CNAs including deletions of 16q22 and 16q24

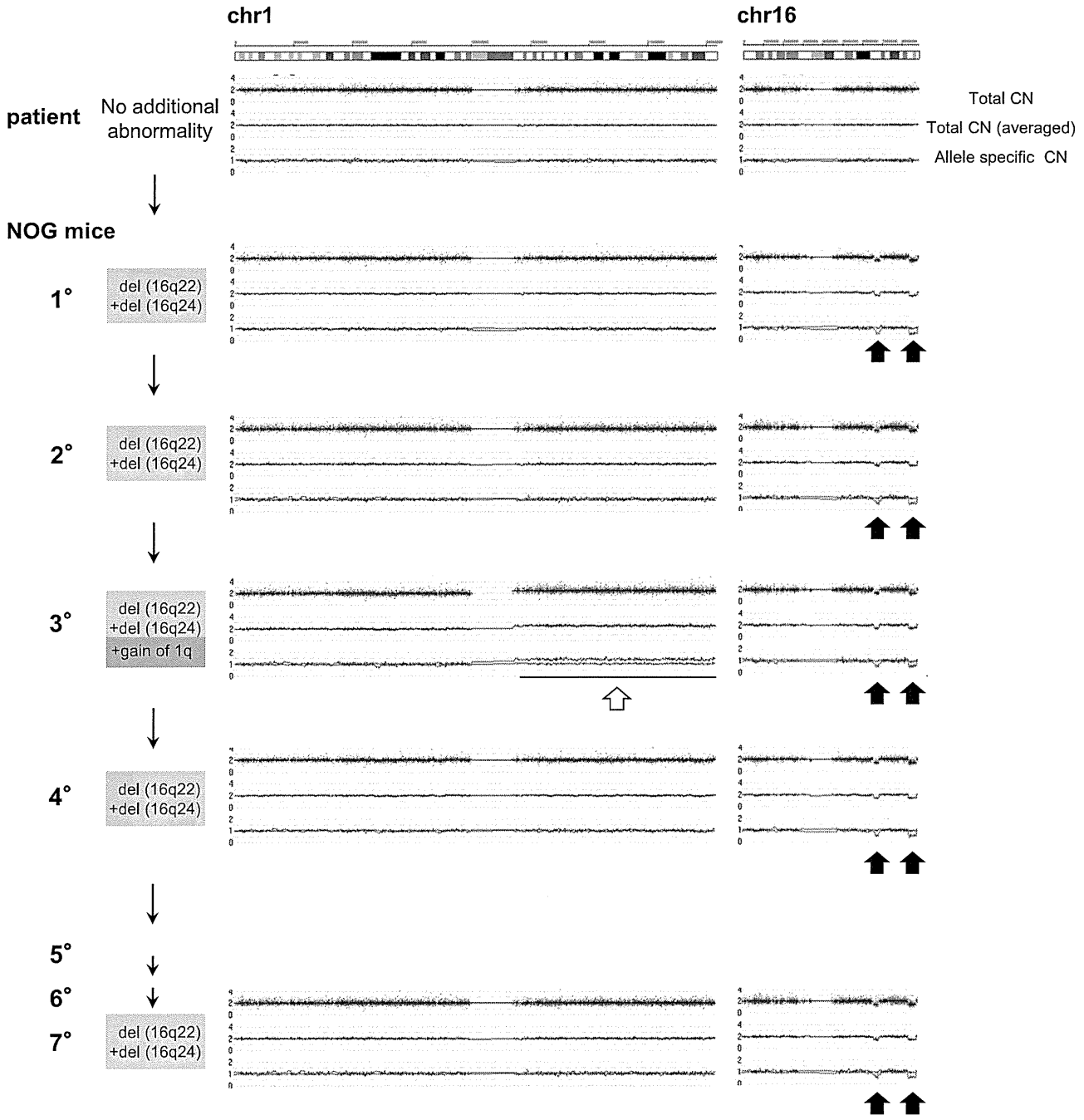

Figure 3. Sequential CNA analysis of TAM-derived cells in the recipients of patient 1. DNA obtained from the original patient sample and sorted hCD45$^+$ recipient BM cells were analyzed by Affymetrix GeneChip Mapping 250K arrays and compared with the PB sample of the original patient in complete remission phase. The primary sample of the patient in TAM phase (blast 92%) had no CNA. hCD45$^+$ BM cells of 1° to 7° recipients had a hemi-allelic deletion in regions 16q22 and 16q24 (black arrows). The 3° recipient had a gain of the entire arm of chromosome 1q (white arrow) in addition to deletion of 16q22 and 16q24. Arrowhead indicates abnormal CNA.

(Figure 4A). To determine whether these subclones were present at low levels in the primary sample of patient 1, specific PCR for the 16q22 deletion was performed using primer pairs designed to bookend the deletion site. CNA analysis and genome sequencing data in these deletion sites (16q22 and 16q24) revealed the presence of genomic breakage and inversion (Figure 5A; supplemental Figures 3 and 4; see supplemental Methods for details). A primer set was designed to detect the deduced breakpoint and used to perform PCR on TAM-derived cells from patient 1 in the recipients with 16q22 and 16q24 deletions. PCR using genomic DNA from TAM-derived cells in the 1° to 8° recipients of the first series of transplantations (Figure 3) produced a uniformly bright DNA fragment of the same size, consistent with the results of CNA profiling (Figure 5B). A faint fragment was detected by applying this PCR method to genomic DNA from the primary patient sample (patient 1), which was confirmed to contain the deletion breakpoint in 16q22 by Sanger sequencing. These results demonstrated that TAM cells with the 16q22 and 16q24 deletions already resided as a minor population in the original sample of patient 1. The frequency of the mutant cells was estimated to be ~1.0% to 0.2% of the patient's PBMCs by a serial dilution assay (supplemental Figure 5).

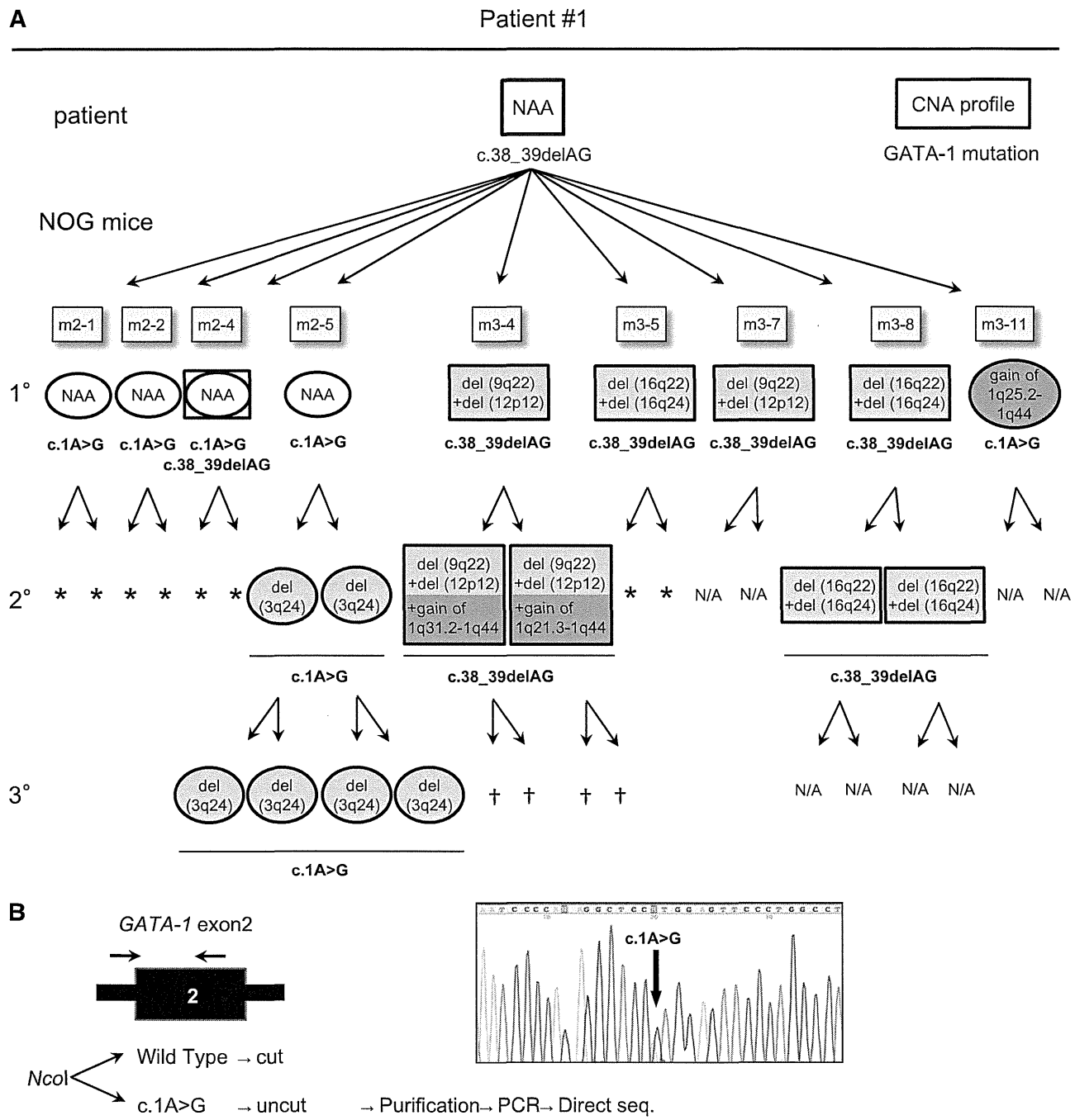

Figure 4. TAM-derived cells show genetic and functional diversity. (A) Summary of the serial transplantation of TAM cells of patient 1 and the results of CNA profiling and *GATA1* mutation analysis. The original patient sample had a single *GATA1* mutation, c.38G_39delAG, and no additional CNAs. Diverse subpopulations with or without additional CNAs expanded in each recipient. *GATA1* mutation analysis showed 2 distinct mutations in recipients: one identical to that of the original patient (c.38_39delAG) and a different mutation (c.1A>G). The mice harboring cells with the original mutation (c.38_39delAG) are shown in rectangles, and the mice with cells harboring the other mutation (c.1A>G) are shown in ovals, with a CNA profile note inside. The *GATA1* mutation is indicated below the symbol. NAA, no additional alteration; N/A, not assessed because of low blast cell count. †Death of recipient before analysis. *No engraftment. (B) Detection of a minor clone with the c.1A>G mutation in the original sample of patient 1. NcoI digestion of a DNA fragment obtained by PCR of *GATA1* exon 2 yielded 2 fragments in the wild type, whereas the mutant allele (c.1A>G) remained undigested. PCR of the undigested band and direct sequence analysis identified the same *GATA1* mutation (c.1A>G mutation) in the patient sample. Black arrow indicates the primer set.

The same method was used to detect a subclone with a 3q24 deletion in the primary patient sample (m2-5; Figure 4A; supplemental Figure 6). At the site of the deletion, genomic breakage was confirmed, and the ends were bound by insertion of a G-nucleotide (Figure 5C; supplemental Figure 7). Consistent with the results of CNA profiling, PCR using DNA from engrafted cells in the 2° and 3° mice (m2-5; Figure 4A) produced a bright DNA fragment, which was confirmed to contain the deletion breakpoint in 3q24 by Sanger sequencing (Figure 5D). Engrafted cells from the BM of the 1° recipient produced a faint DNA fragment, although CNAs were not detected in these cells by array-based methods. We could not detect the corresponding DNA fragment in the primary sample of patient 1. These results suggest the subclone with the 3q24 deletion arose in the 1° recipient mouse as a minor population, emerged as a major population in the 2° recipient, and subsequently engrafted into the 3° recipients.

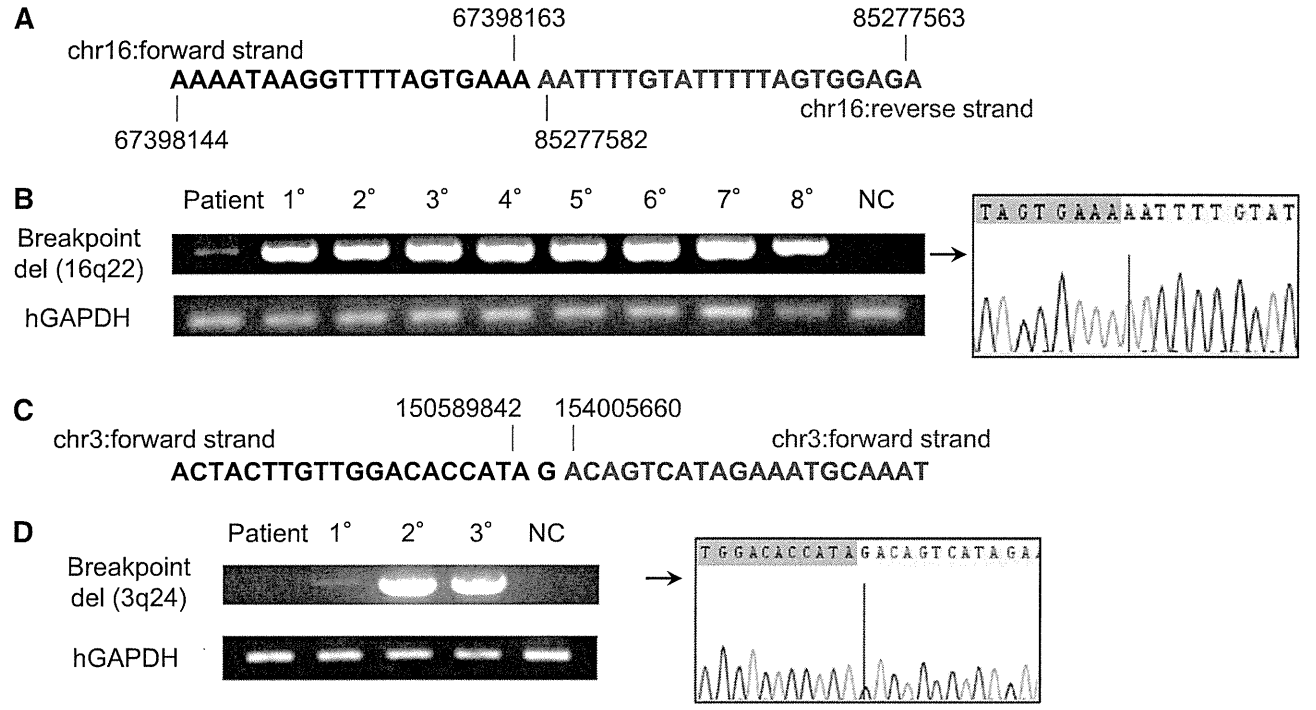

Figure 5. A minor subclone with additional CNAs was present in the primary TAM patient sample, whereas a new clone emerged in a 1° recipient. (A) Contig of del (16q22) breakpoint deduced by whole genome sequencing of the clone containing del(16q22) and del(16q24) in patient 1. Details are shown in supplemental Figure 6. (B) Breakpoint-specific PCR for the del(16q22) clone using genomic DNA from the original patient sample (1; PB in TAM phase), 1° to 8° xenografts (hCD45$^+$ BM cells; Figure 3), and NC (negative control; PBMCs from a healthy adult). Cells from 1° to 8° recipients showed a bright band. The original patient sample showed a faint band, and direct sequencing revealed the presence of the deduced breakpoint for del(16q22). Human glyceraldehyde-3-phosphate dehydrogenase (hGAPDH) was used as an internal control. (C) Contig of del(3q24) breakpoint deduced by whole-genome sequencing. Details are shown in supplemental Figure 9. (D) Breakpoint-specific PCR for the del(3q24) clone using genomic DNA from the original patient sample (1; PB in TAM phase), 1° to 3° xenografts (hCD45$^+$ BM cells, m2–5; Figure 4A), and NC. Cells from 2° and 3° recipients showed a bright band. No band was detected in the original patient sample, but a faint band was detected in the 1° recipient sample. hGAPDH was used as an internal control. Direct sequencing confirmed the presence of cells with the deduced breakpoint for del(3q24) in the 1° recipient.

However, because the sensitivity of the specific PCR targeting of the 3q24 deletion was ~0.1% as determined by the dilution assay (data not shown), it is also possible that this minor clone already existed in the primary patient sample at a frequency below the sensitivity limit. Collectively, our results provide evidence that subclones with additional genetic alterations already exist in the TAM phase and suggest that clonal selection occurs continuously in this xenograft model.

TAM cells derived from patients who did not develop ML-DS had limited self-renewal capacity and fewer additional CNAs than those from the patient who developed ML-DS

To assess whether TAM cells derived from the patients who did not develop ML-DS had similar self-renewal capacity and genetic instability to those from patient 1, CNA analysis of TAM-derived cells was performed by transplanting the preserved PBMC samples of patients 2 and 9. In patient 2, 4 1° transplantation attempts resulted in successful engraftment. The primary sample of patient 2 had no CNAs (Figure 6A). However, TAM-derived cells in 1 of the 1° recipients (m2-2) showed 7p and 7q deletions, suggesting that a subclone with these CNAs may exist in the primary patient sample. The other 2 1° recipients had no additional CNAs (m2-1 and m3-6). In patient 9, engraftment succeeded in 5 1° recipients, and no additional CNAs were detected in either primary patient sample or engrafted TAM-derived cells (Figure 6B). The engrafted cells in all of the recipient mice harbored the same *GATA1* mutation as that of the primary samples of patients 2 and 9. In these 2 cases, our xenograft assay did not detect potent TAM clones with self-renewal capacity in serial transplantation assays (Figure 6A-B; supplemental Table 1), which may reflect the favorable clinical outcome of these patients.

Taken together, the results show that only the TAM cells derived from patients who subsequently developed ML-DS had long-term self-renewal capacity with additional CNAs in our serial transplantation assay.

Discussion

New genomic technologies have led to a better understanding of the complex clonal architecture of leukemia and have shown that disease progression occurs through clonal evolution.[20-22,32] However, most studies have been based on the retrospective analysis of frank leukemia samples, and data on the evolutionary process occurring in the preleukemic phase are limited because primary preleukemia samples are rarely available and are difficult to maintain in vitro or in vivo. TAM is a unique hematologic condition associated with DS that is mostly self-limited but leads to ML-DS in 20% of cases after spontaneous remission. Therefore, TAM has been considered a preleukemic state and is a suitable pathological condition to analyze the evolutionary process of leukemia.

Because mice models in which primary human leukemic cells were transplanted into immunodeficient hosts provided significant clues to advance our understanding of the pathogenesis of human

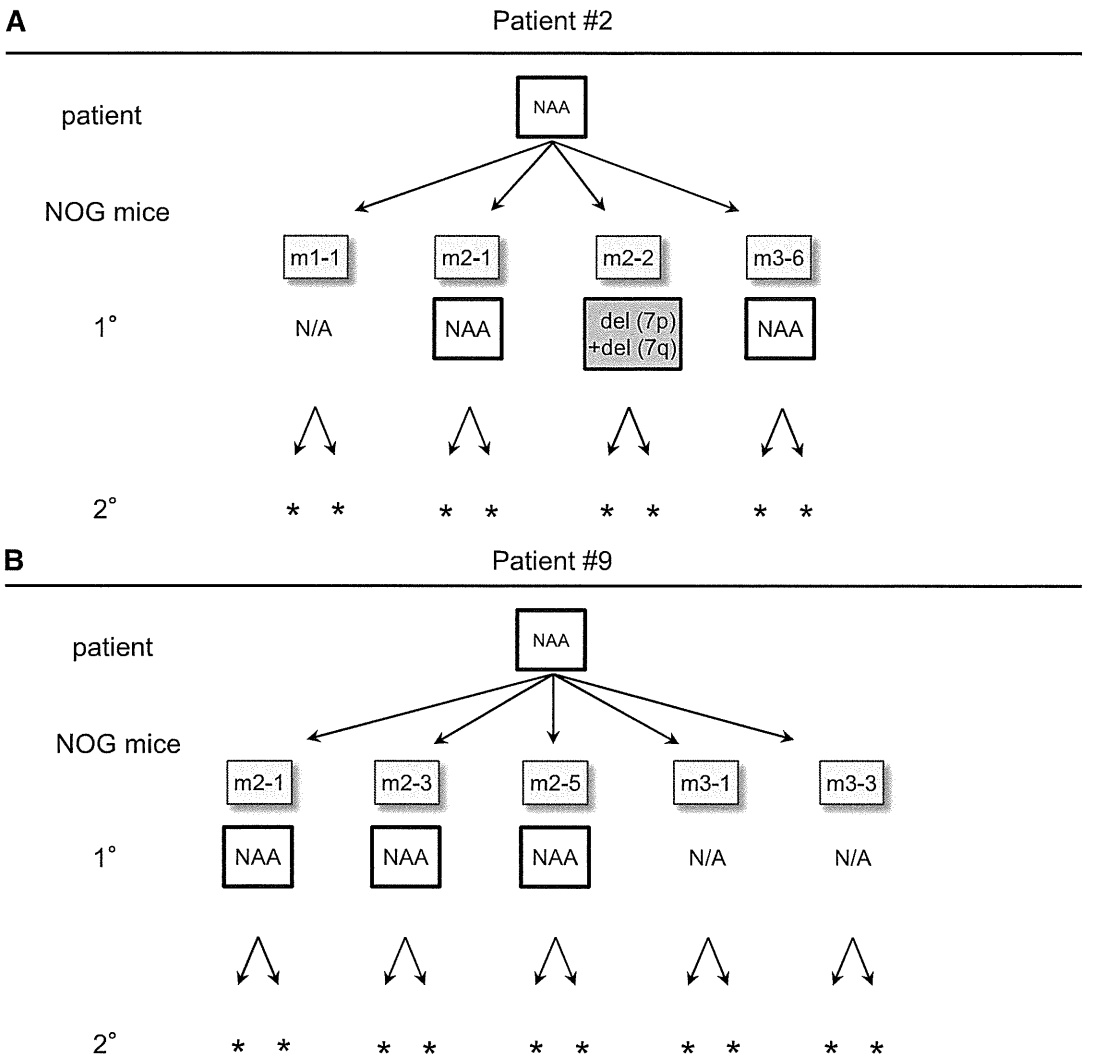

Figure 6. Serial transplantation and CNA profiling of TAM-derived cells from patients that did not develop ML-DS. (A) Serial transplantation assay using TAM cells from patient 2. Four attempts resulted in successful analysis in 1° recipients. CNAs with del(7p) and del(7q) were observed in 1 recipient (m2-2). No additional CNAs were observed in any other recipients. No engraftment was observed in 2° recipients. (B) Serial transplantation assay of TAM cells from patient 9. Five attempts resulted in successful analysis in 1° recipients. No additional CNAs were observed in any analyzed recipients, and no engraftment was observed in 2° recipients. NAA, no additional alteration; N/A, not assessed because of low cell count. *No engraftment.

leukemia,[19-22] we hypothesized that xenograft models of TAM cells would be an attractive method to investigate leukemogenesis. In this report, we demonstrated the long-term engraftment of primary TAM cells in NOG mice and showed that TAM cells from a patient that subsequently developed ML-DS had the potential to gain diverse additional genomic alterations and self-renewal capacity. Although we were unable to determine whether the clonal evolution of TAM cells observed in our model reflected the clinical phenotype of the original patient because of insufficient sample from the ML-DS phase, our model is likely to enable the prospective evaluation of leukemic evolution and can be a powerful tool to study the pathophysiology of leukemogenesis. Our model using NOG mice contrasts somewhat with the study by Chen et al,[27] who reported that TAM cells resided only in the BM after intra-BM infusion into NOD/SCID mice. We speculate that a severe and unique immunodeficient microenvironment may have contributed to the successful engraftment of TAM cells in NOG mice.

In the present study, primary TAM cell samples from 3 of 11 patients engrafted in NOG mice (Figure 1), but serial engraftment was successful only with cells obtained from the patient who developed ML-DS at the age of 1 year (Figures 2, 3, and 6). The results of extensive serial transplantation revealed the emergence of subclones with various additional CNAs characteristic of ML-DS (Figures 3 and 4). Furthermore, we showed that minor subclones with various CNAs and a distinct *GATA1* mutation were already present in the ML-DS patient during the early TAM phase (Figures 4 and 5), as previously described for polyclonality of TAM.[2,33] These findings suggest that several preleukemic clones with high leukemia-initiating potential may already reside as minor clones in TAM cells of patients fated to develop ML-DS and show high repopulating capacity in the special microenvironment of NOG mice. Our findings support the hypothesis that ML-DS develops from a pool of heterogeneous minor clones through clonal selection, illustrating the early evolutionary process of leukemia.[34]

Long-term engraftment of TAM-derived cells was observed for only a minority of TAM patients. This finding suggests that factors other than the properties of the TAM-derived cells, such as technical issues, affected engraftment efficiency. In this regard, increasing the number of transplanted cells resulted in a higher rate of engraftment in recipients of samples from patient 9 (supplemental Table 1).

However, there was no clear association between the percentage of TAM blast cells in transplanted samples and successful engraftment (supplemental Table 1). Likewise, frozen samples from 3 patient samples (patients 1, 2, and 9) were as efficient for engraftment as fresh samples from these patients. Therefore, although the number of injected TAM cells and technical issues may affect engraftment, we speculate that engraftment efficiency is an intrinsic property of each TAM-derived cell population.

In addition to trisomy 21, somatic *GATA1* mutation is considered an early essential event of TAM and ML-DS occurring in utero.[35,36] Interestingly, our TAM-NOG mice model enhanced the emergence of a minor clone with a distinct *GATA1* mutation that was not detectable in the original patient sample by conventional sequencing methods. In our model, a minor *GATA1* mutant clone expanded predominantly in some recipients and acquired CNAs independently of clones with the original *GATA1* mutation, raising the possibility that leukemic evolution occurred from this minor clone, similar to the clinical observation in our previous report.[13] In this scenario, a common founder clone of TAM/ML-DS may be established before the acquisition of the *GATA1* mutation, or TAM clones with distinct *GATA1* mutations may arise independently in the fetal period.

It has long been considered that the linear sequential acquisition of genetic alterations induces disease progression in TAM/ML-DS.[37] By contrast, recent studies using high-throughput genomic technology indicate that evolutionary trajectories are more complex and branching in other cancers and leukemias, as previously proposed by Nowell.[38] In this theory, genomic instability in founder cells gives rise to heterogeneous mutant subclones, and under selective pressure, some subclones expand to result in disease progression, whereas others become extinct or remain dormant. Thus, leukemic clones may evolve and emerge through the complex interaction of selectively advantageous "driver" mutations, additional advantageous "cooperating" mutations, neutral "passenger" mutations, and deleterious mutations.[32,38] It is clinically true that genomic alterations are more frequently observed in ML-DS than in TAM.[2,11,39] In this paper, we showed that diverse subclones with various CNAs can be generated in TAM, and these events occurred preferentially in a patient who later developed ML-DS. These findings suggest the presence of leukemic driver mutations in the early phase of TAM in this patient, which may have induced genomic instability. We were unable to find any candidate tumor-associated genes on the deletion sites (3q24, 9q22, 12p12, 16q22, and 16q24) of TAM-derived cells using the The National Center for Biotechnology Information database, suggesting that other genetic mutations and epigenetic events may contribute to the progression to ML-DS, including a few candidate mutations identified previously.[40-42] It is also noteworthy that subclones in each recipient mouse showed different repopulating capacities in this study. The dominant clones in each recipient were not always identical in the 1° generations, and the dominant clone in a certain recipient did not always propagate dominantly in the next generation recipients (Figure 4A). Differences between the recipient mice or technical problems may have caused variations in engraftment outcome, which is a potential weakness of this xenograft model; however, it is more likely that cooperating genetic event(s) important for leukemogenesis led to the cells of a specific TAM clone becoming the dominant population in each recipient. Such cooperating event(s) could have a considerable impact on a preleukemic TAM clone, and clonal selection might occur in a somewhat random manner. Thus, leukemic evolution may depend on random chance to an extent. Our TAM xenograft model may help demonstrate the branching architecture of clonal evolution in a preleukemic phase, which contrasts with a linear and deterministic pattern of evolution.[34,38] Further genomewide analysis is needed to elucidate the true driver or cooperating mutation(s) and unravel the evolutionary process of leukemia.

In conclusion, we established a xenograft model of TAM using highly immunodeficient NOG mice. Our model enabled the observation of clonal selection and expansion of minor mutant TAM clones and is likely to mimic the early phase of the leukemic evolutionary process, demonstrating the striking genetic heterogeneity and the propagating potential of minor clones in a preleukemic phase. Our xenograft model could be valuable tool for gaining insight into the leukemogenesis of ML-DS and for evaluating the prognosis of TAM patients.

Acknowledgments

The authors thank all the TAM patients and their families for their participation. The authors thank Drs Akira Niwa, Masashi Sanada, Hironao Numabe, Tomoki Kawai, Takahiro Yasumi, and Ryuta Nishikomori for technical advice.

This work was supported by grants from the Japanese Ministry of Education, Culture, Sports, Science, and Technology, and from the Japanese Ministry of Health, Labor and Welfare.

Authorship

Contribution: S.S., I.K., T.M., H.F., and K.U. performed sample collection and processing; S.S., K.T., K.Y., and R.W. performed experiments; A.S.-O. performed microarray analysis (accession number GSE44739); Y.S. and S.M. provided expert statistical analysis; S.S., Y.O., and T.T. analyzed results and made the figures; M.I. and T.N. generated NOG mice; and S.S., K.W., H.H., S.A., E.I., S.O., and T.H. designed the research and wrote the paper.

Conflict-of-interest disclosure: The authors declare no competing financial interests.

Correspondence: Toshio Heike, Department of Pediatrics, Graduate School of Medicine, Kyoto University, 54 Kawaharacho, Shogoin, Sakyo-ku, Kyoto, 606-8507, Japan; e-mail: heike@kuhp.kyoto-u.ac.jp.

References

1. Pine SR, Guo Q, Yin C, Jayabose S, Druschel CM, Sandoval C. Incidence and clinical implications of GATA1 mutations in newborns with Down syndrome. *Blood.* 2007;110(6):2128-2131.
2. Massey GV, Zipursky A, Chang MN, et al; Children's Oncology Group (COG). A prospective study of the natural history of transient leukemia (TL) in neonates with Down syndrome (DS): Children's Oncology Group (COG) study POG-9481. *Blood.* 2006;107(12):4606-4613.
3. Zipursky A, Poon A, Doyle J. Leukemia in Down syndrome: a review. *Pediatr Hematol Oncol.* 1992;9(2):139-149.
4. Hitzler JK. Acute megakaryoblastic leukemia in Down syndrome. *Pediatr Blood Cancer.* 2007;49(7 Suppl):1066-1069.
5. Hitzler JK, Cheung J, Li Y, Scherer SW, Zipursky A. GATA1 mutations in transient leukemia and acute megakaryoblastic leukemia of Down syndrome. *Blood.* 2003;101(11):4301-4304.
6. Wechsler J, Greene M, McDevitt MA, Anastasi J, Karp JE, Le Beau MM, Crispino JD. Acquired mutations in GATA1 in the megakaryoblastic leukemia of Down syndrome. *Nat Genet.* 2002;32(1):148-152.